

On the whole spectrum of Timoshenko beams. Part I: a theoretical revisit

Antonio Cazzani, Flavio Stochino and Emilio Turco

Abstract. The problem of free vibrations of the Timoshenko beam model is here addressed. A careful analysis of the governing equations allows identifying that the vibration spectrum consists of two parts, separated by a *transition frequency*, which, depending on the applied boundary conditions, might be itself part of the spectrum. For both parts of the spectrum the values of natural frequencies are computed and the expressions of eigenmodes are provided: this allows to acknowledge that the nature of vibration modes changes when moving across the transition frequency. Among all possible combination of end constraints which can be applied to single-span beams, the case of a simply supported beam is considered. These theoretical results can be used as benchmarks for assessing the correctness of the numerical values provided by several numerical techniques, *e.g.* traditional Lagrangian-based finite element models, or the newly developed Isogeometric approach.

Mathematics Subject Classification (2010). Primary 74K10, 74H45, 74H05; Secondary 70J10, 70J30, 34L10, 34L15, 35C05, 35L25.

Keywords. Structural dynamics, Vibration analysis, Timoshenko beam, Frequency spectrum.

1. Introduction

A beam model which is able to take into account both shear stiffness and rotary inertia (in addition to bending stiffness and transversal inertia, which are typical of the Euler-Bernoulli model) for structural dynamics applications was first proposed by Timoshenko in 1921 [1] and further developed in 1922 [2] and since then it is associated to his name. A previous attempt to extend the Euler-Bernoulli [3] model by incorporating in it rotary inertia alone is ascribed to Rayleigh [4]. Together with the so called *shear beam* model, which descends from Timoshenko model by disregarding in it the rotary inertia contribution, these four beam models constitute the theoretical background for standard structural mechanics applications, when second- or higher-order effects can be neglected and hence there is no coupling between transversal and longitudinal vibrations. An interesting overview of these theories and a comparison of their applications in structural problems of engineering interest is presented in [5], while in [6] a comparison of Euler-Bernoulli and Timoshenko models with a 2-D elasticity solution is proposed. On the other hand, a variational formulation of the Timoshenko beam model has been proposed in [7] and in [8], while a study of nonlinear vibrations has been reported in [9].

Despite the large number of papers which have appeared since 1921 on the dynamics of Timoshenko beam, there are still some issues which deserve some attention, in particular a complete and precise definition of the vibration spectrum. There is indeed much confusion about it, and several contributions, instead of helping in clarifying the topic have instead added more incomplete pieces of information and misunderstandings. The most debated issue is the so-called *second spectrum* of Timoshenko beam theory, which was first described by Traill-Nash and Collar [10]. Following this paper many contributions on this issue appeared; for an updated but inevitably incomplete list, at

22 least the following works should be mentioned (in order of appearance): [11, 12, 13, 14, 15, 16, 17, 18,
23 19, 20, 21, 22, 23, 24, 25].

24 The idea of considering two spectra for the Timoshenko beam can be justified and acceptable in
25 the framework of wave propagation, but, as long as structural vibrations are envisaged, can lead to
26 serious misunderstandings. Indeed, looking carefully at the governing equations of motion, as it has
27 been attempted in [26], it follows that there is a unique vibration spectrum, but with a transition
28 between two different kinds of vibration modes. Disregarding one part of the spectrum, as some
29 authors have claimed to do, with the motivation that it is physically unfeasible leads to contradictory
30 conclusions. Indeed only mechanical experiments can be used to validate a theory and in the case that
31 experimental results do not match with the theoretical model, the latter has to be changed. Instead
32 numerical codes implementing the Timoshenko beam model produce results which are inherently
33 coherent with the same theory and cannot be used to validate or reject the theory itself.

34 As a matter of fact, most handbooks concerned with the definition of eigenmodes for the single-
35 span Timoshenko beam model make reference only, regardless of the considered boundary conditions,
36 to the first part of the spectrum: see, for instance, Pilkey [27, pp. 596–ff.] or Reddy [28, pp. 197–200].
37 Disregarding the second part of the spectrum can still be acceptable for relatively slender beams if
38 only the first few vibration modes (*e.g.* less than ten) are required, but for shorter beams this can
39 be unacceptable, since the transition to the second part of the spectrum, when the depth-to-span
40 ratio is less than 5, as Table 2 shows, may occur around the seventh mode. Even in the rare cases
41 when the second part of the spectrum is accounted for, *e.g.* in Karnowsky and Lebed [29, pp. 331-
42 ff.], the provided solution is given in terms of complex-valued functions, which is an unnecessary
43 complication; moreover, for the simply supported beam, the presence of the eigenmode corresponding
44 to the transition frequency has been overlooked.

45 Hence this paper is devoted to carefully developing, using only real-valued variables, the complete
46 solution, in terms of natural frequencies and corresponding vibration modes, for the Timoshenko beam
47 in the most general case. Results are then specialized to some peculiar boundary conditions: for these
48 cases, the numerical values of natural frequencies and eigenmodes are constructed. These theoretical
49 results will then be used, in a forthcoming paper, [30] as suitable benchmarks to assess, from a
50 quantitative point of view, the accuracy exhibited by some finite element models.

51 The rest of the paper is organized as follows: in Section 2 the governing equations of the dynamics
52 of a straight Timoshenko beam are presented: in particular the decoupled fourth-order differential
53 equations for the two components of the generalized displacement are deduced and solved. Discussion
54 is then focused on the eigensolutions: it is shown that their nature changes when passing through
55 a transition frequency, so that the spectrum, composed of those particular frequency values such
56 that vibration are possible, consists of two parts with, eventually, the addition of the special value
57 corresponding to the transition frequency. It has to be remarked that the analysis of the eigensolutions
58 is performed in order to deal only with real-valued functions.

59 Then, in Section 3 modal analysis for the single-span Timoshenko beam model is presented for the
60 simply supported beam. This is the simplest case, which has been extensively studied in the literature,
61 and is characterized by a factorized form of the transcendental equation providing the wave-numbers
62 associated to natural vibrations. This circumstance allows to obtain a *closed-form* expression for the
63 vibration frequencies, and produces very simple vibration modes for both part of the spectrum, as well
64 as for the transition frequency, which is indeed part of the spectrum itself. For the analysed case, the
65 complete list of the first 50 natural frequencies is given for suitably chosen geometric and material data,
66 as well as some representative plots of the eigenmodes in different portions of the spectrum; moreover
67 a comparison between the spectrum of the Euler-Bernoulli model and that of the Timoshenko one is
68 presented for the same geometric and material data.

69 Finally in Section 4 some conclusions are drawn, and possible applications of the present research
70 are exemplified. After this, some Appendices illustrate subtler details of the formulation, which have
71 been omitted, for the sake of conciseness, from the main body of the paper.

72 A complete list of symbols is here provided for the reader's convenience.

Symbol	Definition
A	coefficient matrix for the homogenous system
X	unknown column matrix for the homogenous system
0	right-hand side column matrix for homogeneous system
A	cross section area
A_1, A_2, A_3, A_4	integration constants for V , first part of the spectrum
B	cross section depth (and width)
$B_1, B_2, B_3, B_4,$	integration constants for Φ , first part of the spectrum
C_1, C_2, C_3, C_4	integration constants for V , transition frequency
D	constant factor (see Eq. (B.3))
D^*	differential operator d/dx
D_1, D_2, D_3, D_4	integration constants for Φ , transition frequency
E	Young's modulus
E_1, E_2, E_3, E_4	integration constants for V , second part of the spectrum
$E_{1n}, E_{2n}, E_{3n}, E_{4n}$	integration constants for the n -th eigenmode
F_1, F_2, F_3, F_4	integration constants for Φ , second part of the spectrum
G	shear modulus
H, K	amplitude of eigenmodes for double eigenvalue
I	cross section mass moment of inertia
L	beam length
\tilde{L}	special value of beam length
M	bending moment
T	shear force
T^*	differential operator d/dt
V	vibration mode for transversal displacement
a	shear stiffness
b	transversal inertia
\hat{b}, \hat{c}	coefficients of biquadratic wave-numbers equation
b^*, c^*	coefficients of biquadratic frequency equation
c	bending stiffness
d	rotary inertia
f_λ	space frequency associated to wave-number λ
f_{λ_n}	space frequency associated to the n -th vibration mode
k, k_1, k_2	integer values corresponding to wave-numbers of vibration modes
t	time variable
v	transversal displacement
x	space variable (beam abscissa)
$\hat{\Delta}$	discriminant of wave-number equation
Δ^*	discriminant of frequency equation
Φ	vibration mode for section rotation
$\hat{\alpha}_1$	coefficient of eigenmode for generalized wave-number
α_1, α_2	eigenmode coefficients for first/second wave-number
$\tilde{\alpha}_2$	eigenmode coefficient for second wave-number at transition frequency
κ	shear correction factor
$\hat{\lambda}_1$	generalized wave-number (first part of the spectrum)
λ_1	first wave-number (second part of the spectrum)
λ_2	second wave-number (first and second part of the spectrum)
$\tilde{\lambda}_2$	second wave-number at transition frequency

λ_1^{*2}	first root (squared) of wave-numbers equations
λ_2^{*2}	second root (squared) of wave-numbers equations
ν	Poisson's ratio
ξ	dimensionless space variable (dimensionless beam abscissa)
ρ	beam density (mass per unit volume)
ϕ	section rotation
ω	angular frequency
$\tilde{\omega}$	angular frequency at the transition value (cut-off frequency)
ω^*	limiting value (upper/lower bound) for angular frequency
ω_n	angular frequency (theoretical value) for n -th vibration mode

73 2. The governing equations of dynamics for Timoshenko beams

For a uniform, straight Timoshenko beam, the Linear and Angular Momentum Balance equations are respectively:

$$\frac{\partial T}{\partial x} - \rho A \frac{\partial^2 v}{\partial t^2} = 0, \quad (2.1)$$

$$\frac{\partial M}{\partial x} - T - \rho I \frac{\partial^2 \phi}{\partial t^2} = 0, \quad (2.2)$$

74 where T and M stand respectively for the transversal shear force and the bending moment; ρ is
 75 density of the material constituting the beam; A and I are the area and the area moment of inertia
 76 of the beam cross-section, while $v = v(x, t)$ and $\phi = \phi(x, t)$ are the generalized displacement of the
 77 beam, *i.e.* the transversal displacement of the centroid and the cross-section rotation, which depend
 78 on both the abscissa, x , and time, t . It is remarkable that the last terms in the left-hand side of these
 79 Eqs. (2.1)–(2.2) take into account respectively the transversal inertia force and the rotary inertia
 80 torque.

81 The adopted positive convention for internal forces and generalized displacement are shown in
 Figure 1.

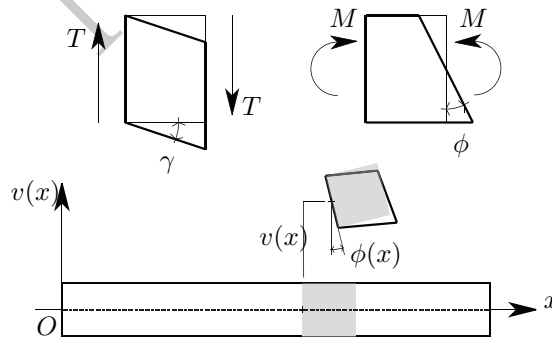


FIGURE 1. Timoshenko beam element showing the assumed conventions for generalized displacements (v , ϕ) and internal forces (T , M).

82
 83 The Constitutive Equations at the beam level, taking into account that G and E are shear and
 84 Young's moduli, and κ is the shear-correction factor, read:

$$T = G\kappa A \left(\frac{\partial v}{\partial x} + \phi \right), \quad M = EI \frac{\partial \phi}{\partial x}, \quad (2.3)$$

and allow, once they are substituted into Eqs. (2.1)–(2.2), to obtain the coupled equations of motion written in terms of kinematic variables alone:

$$G\kappa A \left(\frac{\partial^2 v}{\partial x^2} + \frac{\partial \phi}{\partial x} \right) - \rho A \frac{\partial^2 v}{\partial t^2} = 0, \quad (2.4)$$

$$EI \frac{\partial^2 \phi}{\partial x^2} - G\kappa A \left(\frac{\partial v}{\partial x} + \phi \right) - \rho I \frac{\partial^2 \phi}{\partial t^2} = 0. \quad (2.5)$$

2.1. Fully-decoupled equations of motion

This system of two second-order Partial Differential Equations (PDEs) can be conveniently reduced to a unique fourth-order PDE. Towards this purpose, a symbolic form of Eqs. (2.4)–(2.5) which is suitable for operator calculus can be easily devised by defining the following short-hand notation:

$$a = G\kappa A, \quad b = \rho A, \quad c = EI, \quad d = \rho I. \quad (2.6)$$

Similarly, the following symbols are used to denote the differential operators:

$$D^* = \frac{\partial(\cdot)}{\partial x}, \quad D^{*2} = \frac{\partial^2(\cdot)}{\partial x^2}, \quad \dots, \quad D^{*4} = \frac{\partial^4(\cdot)}{\partial x^4}, \quad (2.7)$$

$$T^* = \frac{\partial(\cdot)}{\partial t}, \quad T^{*2} = \frac{\partial^2(\cdot)}{\partial t^2}, \quad \dots, \quad T^{*4} = \frac{\partial^4(\cdot)}{\partial t^4}. \quad (2.8)$$

In Eqs. (2.6) a and c represent respectively shear and bending stiffness, while b and d are transversal and rotary inertia: the simultaneous presence of all these terms characterizes Timoshenko's beam theory. When some of them are disregarded, other beam theories (*e.g.* those named from Rayleigh or from Euler-Bernoulli or the so-called *shear-beam* theory) are obtained. See, for details [5, 29, 27].

By using the symbolic notation defined above, it results:

$$(aD^{*2} - bT^{*2})v + aD^* \phi = 0, \quad (2.9)$$

$$-aD^* v + (cD^{*2} - a - dT^{*2})\phi = 0. \quad (2.10)$$

By formal operator calculus procedures it follows from Eq. (2.9):

$$aD^* \phi = -(aD^{*2} - bT^{*2})v, \quad (2.11)$$

which allows eliminating ϕ from Eq. (2.10), and yields the following decoupled fourth-order equation in v :

$$acD^{*4}v - (ad + bc)D^{*2}T^{*2}v + abT^{*2}v + bdT^{*4}v = 0. \quad (2.12)$$

After some algebraic manipulations Eq. (2.12) can be written as follows:

$$EI \frac{\partial^4 v}{\partial x^4} - \rho I \left(1 + \frac{E}{G\kappa} \right) \frac{\partial^4 v}{\partial t^2 \partial x^2} + \rho A \frac{\partial^2 v}{\partial t^2} + \frac{\rho^2 I}{G\kappa} \frac{\partial^4 v}{\partial t^4} = 0, \quad (2.13)$$

which is the equation first established by Timoshenko [1] in 1921 when developing a new beam theory able to deal with both shear strain and rotary inertia.

Similarly, if Eq. (2.11) is used this time to eliminate v and the result is substituted again into Eq. (2.10), the following decoupled fourth-order equation in ϕ is obtained:

$$acD^{*4}\phi - (ad + bc)D^{*2}T^{*2}\phi + abT^{*2}\phi + bdT^{*4}\phi = 0, \quad (2.14)$$

which is formally analogous to Eq. (2.12). Hence, with suitable algebraic simplifications, it comes out the fully-decoupled equation of motion in terms of ϕ :

$$EI \frac{\partial^4 \phi}{\partial x^4} - \rho I \left(1 + \frac{E}{G\kappa} \right) \frac{\partial^4 \phi}{\partial t^2 \partial x^2} + \rho A \frac{\partial^2 \phi}{\partial t^2} + \frac{\rho^2 I}{G\kappa} \frac{\partial^4 \phi}{\partial t^4} = 0. \quad (2.15)$$

Remark 1. It has to be emphasized that, since Eqs. (2.13) and (2.15) are equal, as it has been already outlined by Stephen [22] — who used the same notation adopted here — also their solutions have the same form. For this reason in the sequel attention will be focused only on solving Eq. (2.13).

106 2.2. Solutions of the equations of motion

107 Solutions to Eq. (2.13) — or Eq. (2.15) — are sought such that independent variables, *viz.* x and t ,
 108 are separated. In particular it is assumed that time-dependence is of an harmonic kind, so that free
 109 vibrations are possible. Thus,

$$v(x, t) = V(x) \exp(i\omega t), \quad \phi(x, t) = \Phi(x) \exp(i\omega t), \quad (2.16)$$

where $i = \sqrt{-1}$ is the imaginary unit; it follows, consequently, if primes are used to denote derivatives with respect to x :

$$\frac{\partial^4 v}{\partial x^4} = V''''(x) \exp(i\omega t), \quad \frac{\partial^4 v}{\partial t^2 \partial x^2} = -\omega^2 V''(x) \exp(i\omega t), \quad (2.17)$$

$$\frac{\partial^2 v}{\partial t^2} = -\omega^2 V(x) \exp(i\omega t), \quad \frac{\partial^4 v}{\partial t^4} = +\omega^4 V(x) \exp(i\omega t),$$

110 with analogous expressions for the derivatives of $\phi(x, t)$. If Eqs. (2.17) are substituted into Eq. (2.13),
 111 the common time factors are simplified and the coefficient of the highest derivative in the resulting
 112 Ordinary Differential Equation (ODE) is selected to have a unit value, it results:

$$V'''' + \frac{\rho\omega^2}{E} \left(1 + \frac{E}{G\kappa}\right) V'' + \frac{\rho\omega^2}{E} \left(\frac{\rho\omega^2}{G\kappa} - \frac{A}{I}\right) V = 0. \quad (2.18)$$

113 This is a fourth-order ODE with constant coefficients, whose solutions are to be found in the form of
 114 exponential functions $V(x) = \exp(\lambda^* x)$, where, in general, $\lambda^* \in \mathbb{C}$.

115 Then $V'' = \lambda^{*2} \exp(\lambda^* x)$ and $V'''' = \lambda^{*4} \exp(\lambda^* x)$: after substituting these values and performing
 116 some cancelations, this characteristic equation is arrived at:

$$\lambda^{*4} + \hat{b}\lambda^{*2} + \hat{c} = 0, \quad (2.19)$$

i.e. a biquadratic algebraic equation, whose independent variable is λ^* ; for conciseness reasons the following notation has been adopted:

$$\hat{b} = \frac{\rho\omega^2}{E} \left(1 + \frac{E}{G\kappa}\right) = \omega^2 \frac{d}{c} \left(1 + \frac{bc}{ad}\right), \quad (2.20)$$

$$\hat{c} = \frac{\rho\omega^2}{E} \left(\frac{\rho\omega^2}{G\kappa} - \frac{A}{I}\right) = \omega^2 \frac{d}{c} \left(\omega^2 \frac{b}{a} - \frac{b}{d}\right). \quad (2.21)$$

117 The squared roots of Eq. (2.19) are therefore:

$$\lambda_1^{*2} = \frac{1}{2} \left(-\hat{b} + \sqrt{\hat{b}^2 - 4\hat{c}}\right), \quad \lambda_2^{*2} = \frac{1}{2} \left(-\hat{b} - \sqrt{\hat{b}^2 - 4\hat{c}}\right). \quad (2.22)$$

118 2.3. Analysis of the eigensolutions

119 Based on the value of the transition frequency,

$$\tilde{\omega}^2 = \frac{G\kappa A}{\rho I} = \frac{a}{d}, \quad (2.23)$$

120 when solving Eq. (2.19) these three cases must be distinguished, as it is shown in details in Appendix A.

121 **Case 1.** $\omega^2 < \tilde{\omega}^2$. From the analysis presented in Appendix A, for this angular frequency range it
 122 results: $\lambda_1^{*2} > 0$ and $\lambda_2^{*2} < 0$.

123 As a consequence, Eq. (2.19), has *two real roots*, namely $\pm\sqrt{\lambda_1^{*2}}$, and *two purely imaginary*
 124 *conjugate roots*, *viz.* $\pm i\sqrt{-\lambda_2^{*2}}$.

125 **Case 2.** $\omega^2 = \tilde{\omega}^2$. In the present case, by the same analysis developed in Appendix A, it follows:
 126 $\lambda_1^{*2} = 0$ and $\lambda_2^{*2} < 0$. In particular,

$$\lambda_2^{*2} = -\hat{b}|_{\omega^2=\tilde{\omega}^2} = -\left(\frac{G\kappa A}{EI} + \frac{A}{I}\right) = -\left(\frac{a}{c} + \frac{b}{d}\right). \quad (2.24)$$

127 Consequently there is a *null real root*, whose multiplicity is two, and one couple of *imaginary conjugate*
 128 *roots*, namely again $\pm i\sqrt{-\lambda_2^{*2}}$.

129 **Case 3.** $\omega^2 > \tilde{\omega}^2$. This time it results $\lambda_1^{*2} < 0$ and $\lambda_2^{*2} < 0$.

130 As a consequence, *all four roots* of Eq. (2.19) are *purely imaginary*. In particular, there are *two*
 131 *couples of conjugate roots*, i.e. $\pm i\sqrt{-\lambda_1^{*2}}$ and $\pm i\sqrt{-\lambda_2^{*2}}$.

132 **Remark 2.** The value $\tilde{\omega}^2$ given by Eq. (2.23) represents, from the physical point of view, the ratio
 133 between shear stiffness and rotary inertia.

134 Physical reasons show that $G\kappa A > 0$, $\rho I > 0$, so that $\tilde{\omega} = \sqrt{\tilde{\omega}^2} \in \mathbb{R}^+$ and such value can be
 135 attained indeed: it is the value of the *cutoff frequency* of waves propagating in an infinite Timoshenko
 136 beam, as it is shown, for instance, in Graff [31, pp. 185–187].

137 In the analysis presented here, such frequency represents a *transition value* between two different
 138 solutions of the ODE, Eq. (2.18); moreover this transition value might itself be or might be not part
 139 of the frequency spectrum, depending on the applied boundary conditions.

140 2.4. The eigenmodes of Timoshenko beams

141 The analysis developed in Section 2.3 allows identifying, in terms of real-valued quantities only, the
 142 complete solution to Eq. (2.18) and the corresponding equation which provides $\Phi(x)$.

143 Results will be presented separately for the three cases outlined above.

Case 1. $\omega^2 < \tilde{\omega}^2$. The eigenfunctions in terms of $V(x)$ and $\Phi(x)$ are:

$$V(x) = A_1 \cosh \hat{\lambda}_1 x + A_2 \sinh \hat{\lambda}_1 x + A_3 \cos \lambda_2 x + A_4 \sin \lambda_2 x, \quad (2.25)$$

$$\Phi(x) = B_1 \cosh \hat{\lambda}_1 x + B_2 \sinh \hat{\lambda}_1 x + B_3 \cos \lambda_2 x + B_4 \sin \lambda_2 x, \quad (2.26)$$

144 where the following *proper* (λ_2) and *generalized* ($\hat{\lambda}_1$) wave-numbers apply:

$$\hat{\lambda}_1 = +\sqrt{\lambda_1^{*2}}, \quad \lambda_2 = +\sqrt{-\lambda_2^{*2}}. \quad (2.27)$$

145 Indeed, λ_2 , which appears in the argument of a trigonometric function is a *true* wave-number: it gives
 146 the measure of the portion, measured in radians, of sine/cosine waves which appear in a unit length
 147 of the beam. By analogy, $\hat{\lambda}_1$, which is part of the argument of an hyperbolic function (which reduces
 148 to a trigonometric function for imaginary values of its argument) will be defined a *generalized* wave-
 149 number. On the other hand, the number of *complete* sine/cosine waves which appear in a unit length
 150 of the beam define the *space frequency*, $f_\lambda = \lambda/(2\pi)$, as a complete wave has a length equal to 2π .

Looking at Eq. (2.26), it is clear that coefficients B_1, \dots, B_4 depend on A_1, \dots, A_4 because of
 Eq. (2.11), so that after some lengthy algebra it results:

$$\begin{aligned} \Phi(x) = & -\frac{\hat{\alpha}_1}{\hat{\lambda}_1}(A_2 \cosh \hat{\lambda}_1 x + A_1 \sinh \hat{\lambda}_1 x) + \\ & + \frac{\alpha_2}{\lambda_2}(A_4 \cos \lambda_2 x - A_3 \sin \lambda_2 x). \end{aligned} \quad (2.28)$$

151 In Eq. (2.28) the following short-hand notation has been adopted:

$$\hat{\alpha}_1 = \omega^2 \frac{b}{a} + \hat{\lambda}_1^2, \quad \alpha_2 = \omega^2 \frac{b}{a} - \lambda_2^2. \quad (2.29)$$

152 **Case 2.** $\omega^2 = \tilde{\omega}^2$. Since in this case $\lambda_1^{*2} = 0$, $\lambda_2^{*2} = -\tilde{\lambda}_2^2$ it follows that, see Eqs. (2.6) and (2.24):

$$\tilde{\lambda}_2 = \sqrt{\left(\frac{G\kappa A}{EI} + \frac{A}{I}\right)} = \sqrt{\left(\frac{a}{c} + \frac{b}{d}\right)}. \quad (2.30)$$

Then the eigenfunctions have these expressions:

$$V(x) = C_1 + C_2 \frac{x}{L} + C_3 \cos \tilde{\lambda}_2 x + C_4 \sin \tilde{\lambda}_2 x, \quad (2.31)$$

$$\Phi(x) = D_1 + C_2 \frac{x}{L} + D_3 \cos \tilde{\lambda}_2 x + D_4 \sin \tilde{\lambda}_2 x, \quad (2.32)$$

153 where L is the beam length: in this way all coefficients C_1, \dots, C_4 (and, similarly, D_1, \dots, D_4) are
154 dimensionally homogeneous, as in the previous case, see Eqs. (2.25)–(2.26). However, in the present
155 case, there is only one wave-number, namely $\tilde{\lambda}_2$.

Again, the coefficients appearing in Eqs. (2.31)–(2.32) are not independent, since Eqs. (2.9)–
(2.10) hold. By making again use of Eq. (2.11) it is possible to identify those terms having the same
functional dependence on x . In particular, it results:

$$\begin{aligned} \frac{1}{L}D_2 + \tilde{\omega}^2 \frac{b}{a}C_1 &= 0, & \tilde{\omega}^2 \frac{b}{a} \frac{1}{L}C_2 &= 0, \\ \tilde{\lambda}_2(D_4 - \tilde{\lambda}_2 C_3) + \tilde{\omega}^2 \frac{b}{a}C_3 &= 0, & \tilde{\lambda}_2(D_3 + \tilde{\lambda}_2 C_4) - \tilde{\omega}^2 \frac{b}{a}C_4 &= 0. \end{aligned}$$

156 Therefore, these are the explicit links between the two sets of coefficients:

$$D_2 = -\tilde{\omega}^2 \frac{b}{a}C_1 L, \quad C_2 = 0, \quad D_3 = \frac{\tilde{\alpha}_2}{\tilde{\lambda}_2}C_4, \quad D_4 = -\frac{\tilde{\alpha}_2}{\tilde{\lambda}_2}C_3, \quad (2.33)$$

157 where, for the seek of a compact notation, the following definition has been adopted — see also
158 Eqs. (2.23), (2.30):

$$\tilde{\alpha}_2 = \tilde{\omega}^2 \frac{b}{a} - \tilde{\lambda}_2^2 = -\frac{a}{c}. \quad (2.34)$$

Therefore, in the present case, the complete solution in terms of eigenmodes is:

$$V(x) = C_1 + C_3 \cos \tilde{\lambda}_2 x + C_4 \sin \tilde{\lambda}_2 x, \quad (2.35)$$

$$\Phi(x) = D_1 - \tilde{\omega}^2 \frac{b}{a}C_1 x - \frac{\tilde{\alpha}_2}{\tilde{\lambda}_2}(C_3 \sin \tilde{\lambda}_2 x - C_4 \cos \tilde{\lambda}_2 x). \quad (2.36)$$

159 **Remark 3.** The complete solution of the ODEs which define $V(x)$ and $\Phi(x)$ must depend only on
160 *four* independent coefficients, since these equations descend from a system of two second-order PDEs,
161 Eqs.(2.4)–(2.5). This, however, does not require that *both* V and Φ *have to depend on four coefficients*
162 *each*, as it is clearly shown in Eqs. (2.35)–(2.36). In particular, the circumstance that $C_2 = 0$ follows
163 directly from the kinematic condition expressed by Eq. (2.11).

164 On the other hand, if Eq. (2.10) is used instead of Eq. (2.9), it can be easily checked that while the
165 same conditions given by Eqs. (2.33) are recovered for C_2, D_3, D_4 , the value of D_2 remains undefined,
166 since $V(x)$ appears in Eq. (2.10) only with its first derivative with respect to x and, consequently,
167 coefficient C_1 does not appear explicitly.

Case 3. $\omega^2 > \tilde{\omega}^2$. In this last case the eigenfunctions are:

$$V(x) = E_1 \cos \lambda_1 x + E_2 \sin \lambda_1 x + E_3 \cos \lambda_2 x + E_4 \sin \lambda_2 x, \quad (2.37)$$

$$\Phi(x) = F_1 \cos \lambda_1 x + F_2 \sin \lambda_1 x + F_3 \cos \lambda_2 x + F_4 \sin \lambda_2 x, \quad (2.38)$$

168 where the two independent, real-valued wave-numbers are given by:

$$\lambda_1 = +\sqrt{-\lambda_1^{*2}}, \quad \lambda_2 = +\sqrt{-\lambda_2^{*2}}. \quad (2.39)$$

169 Again, coefficients F_1, \dots, F_4 depend on E_1, \dots, E_4 because of Eq. (2.11), so that, after some algebraic
 170 manipulations one gets:

$$\Phi(x) = \frac{\alpha_1}{\lambda_1}(E_2 \cos \lambda_1 x - E_1 \sin \lambda_1 x) + \frac{\alpha_2}{\lambda_2}(E_4 \cos \lambda_2 x - E_3 \sin \lambda_2 x), \quad (2.40)$$

171 where the following short-hand notation has been adopted:

$$\alpha_1 = \omega^2 \frac{b}{a} - \lambda_1^2, \quad (2.41)$$

172 while α_2 is still defined by Eq. (2.29)₂.

173 3. Modal analysis of Timoshenko beams

174 In this Section, modal analysis of a Timoshenko beam is developed, in order to devise its complete
 175 spectrum.

176 The results of Section 2 clearly show that the complete spectrum, *regardless of the boundary*
 177 *conditions*, must be constructed by taking into account that it consists of two portions, *none of which*
 178 *can be disregarded*.

179 In the first part of the spectrum, which is relevant to natural frequencies $\omega_n < \tilde{\omega}$ the eigenmodes
 180 are given, in general, by a linear combination of hyperbolic and trigonometric functions, see Eqs. (2.25)
 181 and (2.28). Only for particular choices of Boundary Conditions (BCs) it is possible to annihilate the
 182 contribution of hyperbolic functions: this happens, for instance, in the case of a simply supported
 183 beam.

184 In the second part of the spectrum, corresponding to natural frequencies $\omega_n > \tilde{\omega}$ modal shapes are
 185 instead given by a linear combination of trigonometric functions having two different wave-numbers,
 186 λ_1 and λ_2 , as Eqs. (2.37) and (2.40) show. Again, in general, these eigenmodes involve both λ_1 and
 187 λ_2 , since wave-numbers are entwined (or even entangled); only for particular cases, *e.g.* the simply
 188 supported beam, the contributions of wave-numbers become decoupled.

189 Moreover, even the transition frequency, $\tilde{\omega}$ might belong to the spectrum, and hence this condition
 190 has to be taken into account, too. If the transition frequency is part of the spectrum, modal shapes
 191 are given by a linear combination of trigonometric functions depending *on just one wave-number*, $\tilde{\lambda}_2$
 192 and of a constant function (for V), see Eq. (2.35), or a linear combination of trigonometric functions
 193 and a complete linear polynomial (for Φ), as Eq. (2.36) shows.

194 In any case, the particular blending of the above-mentioned functions which provides the actual
 195 eigenmode depends on the applied BCs.

196 For a single span beam, as long as transversal vibrations only are envisaged, four basic end
 197 constraints might be encountered: clamped (or fixed), free, guided, supported (or hinged). The corre-
 198 sponding constrained variables in the homogeneous case (perfect constraints) as well as the equivalent
 199 kinematic constraints are listed in Table 1.

TABLE 1. Basic end constraints for a single-span Timoshenko beam. A prime indi-
 cates a derivative with respect to x : $\Phi' = d\Phi/dx$; $V' = dV/dx$.

Constraint	Symbol	Constrained variables	Equivalent kinematic constraints
Clamped (or fixed)	C	$V = 0$ and $\Phi = 0$	$V = 0$ and $\Phi = 0$
Free	F	$T = 0$ and $M = 0$	$V' + \Phi = 0$ and $\Phi' = 0$
Guided	G	$T = 0$ and $\Phi = 0$	$V' = 0$ and $\Phi = 0$
Supported (or hinged)	S	$V = 0$ and $M = 0$	$V = 0$ and $\Phi' = 0$

200 With these 4 basic constraints it is possible to devise ten different combinations of single-span con-
 201 strained beams, provided that combinations where the constraints are simply reversed (*e.g.* C-F and F-
 202 G) are counted only once. These are: clamped-clamped (or *doubly clamped*, C-C), clamped-free (C-F),

203 clamped-guided (C-G), clamped-supported (C-S); free-free (F-F), free-guided (F-G), free-supported
 204 (F-S); guided-guided (G-G), guided-supported (G-S); supported-supported (or *simply supported*, S-S).

205 For the sake of simplicity the spectrum will be explicitly computed here only for the simply
 206 supported beam, while in a companion paper [32] the doubly clamped (C-C) beam will be considered:
 207 that is somehow representative of all other cases which can occur.

208 However only in the case of a simply supported beam the wave-number transcendental equation
 209 can be written in a factorized form and, as a consequence, the frequency equation becomes a simple
 210 algebraic equation, *e.g.* Eq.(3.13), and allows for the evaluation of natural frequencies ω_n by a direct
 211 method. Moreover, the simply supported beam is the only case where the transition frequency is
 212 *always* part of the spectrum.

213 Instead, in all the remaining cases, since the wave-number transcendental equation cannot be
 214 written as a product, there is a complete coupling: indeed, in the first part of the spectrum hyperbolic
 215 functions appear in the eigenmodes, while, in the second part of the spectrum, each eigenmode is
 216 represented by a combination of trigonometric functions which depend on *both* wave-numbers. Then,
 217 the computation of natural frequencies ω_n must be performed by solving a complicated implicit tran-
 218 scendental equation.

219 The transcendental equation corresponding to several other BCs can be found, for instance,
 220 in [14], where only those which are valid for $\omega_n < \tilde{\omega}$ are reported, and in [5], where the complete
 221 expressions are given, although they are written in an unnecessarily involved way.

222 3.1. Material and geometric data

223 Since it is not possible to provide the spectrum of a *generic* Timoshenko beam, attention has been
 224 focused on a particular beam, which from the physical point of view has reasonable (*i.e.* not patho-
 225 logical) geometric and mechanical data. On the other hand, once theoretical details are clear, it is a
 226 simple exercise changing the data to build the spectrum for other simply-supported beams made of
 227 different materials or having different length and/or cross-section shapes.

228 The case which has been analyzed is the following: a straight uniform and homogeneous beam,
 229 whose length is $L = 2$ m, having a square cross-section with side length (either depth or width)
 230 $B = 0.1$ m; as a consequence, the cross-section area and area moment of inertia are respectively
 231 $A = B^2 = 0.01$ m²; $I = B^4/12 = 1/120,000$ m⁴. Moreover, the length-to-depth ratio (a rough
 232 measure of slenderness) is in this case: $L/B = 20$.

233 Material density is assumed to be $\rho = 8000$ kg/m³, Young's modulus $E = 260$ GPa, (*i.e.*
 234 $E = 260 \cdot 10^3$ N/mm²), Poisson's ratio $\nu = 0.3$ so that, under the hypothesis of elastic isotropy, the
 235 shear modulus is $G = 100$ GPa.

236 The last parameter, namely the shear correction factor, has been chosen according to the standard
 237 value (first adopted by Goens in 1931 [33], and based on results obtained by Föppl (1897) [34] with
 238 an elementary strain energy method), given for static analysis of a rectangular cross-section:

$$\kappa = 5/6. \quad (3.1)$$

239 In the literature (see, for further references [35], [36], [37], [38], [39]) for dynamic analyses, a value
 240 depending also on Poisson's ratio has been suggested: in particular for a rectangular cross-section one
 241 should choose either:

$$\kappa = \frac{10(1 + \nu)}{(12 + 11\nu)}, \quad (3.2)$$

242 which was proposed by Cowper (1966) [40], or

$$\kappa = \frac{5(1 + \nu)}{(6 + 5\nu)}. \quad (3.3)$$

243 This was originally proposed in 1957 by Higuchi *et al.* [41] and later endorsed by Hutchinson [42];
 244 according to [43], [44], and [45] it provides a better agreement with 2-D elasticity solutions in the
 245 dynamic range.

It is patent that for a vanishing value of the Poisson's ratio, all the above equation provide the same value, coinciding with Eq. (3.1). Moreover, as a matter of fact, when computing the value of the transition frequency for the considered beam by adopting $\kappa = 5/6$, the value given by Eq. (3.1), the result is $\tilde{\omega} = 111803.39887$ rad/s; for $\kappa = 130/153$, *i.e.* the value provided by Eq. (3.2), the result becomes $\tilde{\omega} = 112894.18957$ rad/s (almost 1% more than the previous one); finally by the last Eq. (3.2), it is $\kappa = 13/15$ and the result changes to $\tilde{\omega} = 114017.54251$ rad/s, *i.e.* less than 2% of the first one: the influence of the choice of κ is really small.

For this reason, and since the interest is that of comparing for *one and the same* problem the theoretical frequency values with those coming out from suitable numerical methods, *e.g.* the traditional displacement-based Finite Element Method (FEM) and the new spline-based Isogeometric Analysis (IGA), without the need of matching experimental results (as it has been done by Rosinger and Ritchie, [46]), there are no particular reasons for preferring for κ the values given by Eqs. (3.2)–(3.3), instead of the simpler one, Eq. (3.1).

3.2. The case of a simply supported beam

For such a beam, whose length is L , the boundary conditions require that (see Table 1):

$$\textcircled{x} = 0 : \quad V = 0 \text{ and } M = 0; \quad \textcircled{x} = L : \quad V = 0 \text{ and } M = 0. \quad (3.4)$$

By virtue of Eq. (2.3)₂ the homogeneous condition $M(x) = 0$ is equivalent to imposing $\Phi'(x) = 0$. It follows then:

1. for $\omega^2 < \tilde{\omega}^2$:

$$\Phi'(x) = -\hat{\alpha}_1(A_1 \cosh \hat{\lambda}_1 x + A_2 \sinh \hat{\lambda}_1 x) - \alpha_2(A_3 \cos \lambda_2 x + A_4 \sin \lambda_2 x). \quad (3.5)$$

2. for $\omega^2 = \tilde{\omega}^2$:

$$\Phi'(x) = -\tilde{\omega}^2 \frac{b}{a} C_1 - \tilde{\alpha}_2(C_3 \cos \tilde{\lambda}_2 x + C_4 \sin \tilde{\lambda}_2 x). \quad (3.6)$$

3. for $\omega^2 > \tilde{\omega}^2$:

$$\Phi'(x) = -\alpha_1(E_1 \cos \lambda_1 x + E_2 \sin \lambda_1 x) - \alpha_2(E_3 \cos \lambda_2 x + E_4 \sin \lambda_2 x). \quad (3.7)$$

In what follows, the two parts of the spectrum and the transition frequency will be treated separately.

3.2.1. First part of the spectrum: $\omega^2 < \tilde{\omega}^2$. When BCs are substituted into Eqs. (2.25) and (3.5), the following homogeneous system of simultaneous linear algebraic equations is obtained:

$$\mathbf{A}\mathbf{X} = \mathbf{0}, \quad (3.8)$$

where the square matrix \mathbf{A} and the column vectors \mathbf{X} and $\mathbf{0}$ have these expressions:

$$\mathbf{A} = \begin{bmatrix} 1 & 0 & 1 & 0 \\ \hat{\alpha}_1 & 0 & \alpha_2 & 0 \\ \cosh \hat{\lambda}_1 L & \sinh \hat{\lambda}_1 L & \cos \lambda_2 L & \sin \lambda_2 L \\ \hat{\alpha}_1 \cosh \hat{\lambda}_1 L & \hat{\alpha}_1 \sinh \hat{\lambda}_1 L & \alpha_2 \cos \lambda_2 L & \alpha_2 \sin \lambda_2 L \end{bmatrix}, \quad \mathbf{X} = \begin{Bmatrix} A_1 \\ A_2 \\ A_3 \\ A_4 \end{Bmatrix}, \quad \mathbf{0} = \begin{Bmatrix} 0 \\ 0 \\ 0 \\ 0 \end{Bmatrix}. \quad (3.9)$$

Since, as a simple check confirms, $\hat{\alpha}_1 - \alpha_2 = \hat{\lambda}_1^2 + \lambda_2^2 > 0$, it follows $A_1 = 0$; $A_3 = 0$ and this reduced system of equations is obtained:

$$\begin{bmatrix} \sinh \hat{\lambda}_1 L & \sin \lambda_2 L \\ \hat{\alpha}_1 \sinh \hat{\lambda}_1 L & \alpha_2 \sin \lambda_2 L \end{bmatrix} \begin{Bmatrix} A_2 \\ A_4 \end{Bmatrix} = \begin{Bmatrix} 0 \\ 0 \end{Bmatrix}. \quad (3.10)$$

Non-trivial solutions to this reduced matrix problem exist provided that $(\alpha_2 - \hat{\alpha}_1) \sinh \hat{\lambda}_1 L \sin \lambda_2 L = 0$, *i.e.* being $\hat{\alpha}_1 - \alpha_2 \neq 0$, when the following transcendental equation is satisfied:

$$\sinh \hat{\lambda}_1 L \sin \lambda_2 L = 0. \quad (3.11)$$

By the rule which ensures the vanishing of a product, it must be:

$$\hat{\lambda}_1 L = 0 \quad \text{or} \quad \lambda_2 L = k_2 \pi, \quad (k_2 \in \mathbb{N}). \quad (3.12)$$

275 The former occurrence has to be disregarded since it implies, for $L \neq 0$ (the alternative $L = 0$ being
 276 unfeasible for physical reasons), by Eq. (2.27)₁ that $\lambda_1^{*2} = 0$ and this only occurs when the natural
 277 frequency is precisely equal to the transition frequency $\omega = \tilde{\omega}$, but then solution is ruled by Case 2,
 278 which is treated below, in Section 3.2.2.

279 The latter occurrence gives, for $L \neq 0$, $\lambda_2 = k_2\pi/L$, and yields (details are given in Appendix B)
 280 the following *frequency equation* for the simply-supported Timoshenko beam:

$$\omega^4 + b^*\omega^2 + c^* = 0. \quad (3.13)$$

281 This Eq. (3.13), which was obtained for the first time in [1], can also be found in [14]: there, however
 282 it has been deduced without a complete discussion like that presented here, and led the authors to
 283 some misleading comments about the second part of the spectrum.

284 Eq. (3.13) is again a biquadratic one, whose squared solutions are:

$$\omega_1^2 = \frac{1}{2}(-b^* + \sqrt{b^{*2} - 4c^*}), \quad \omega_2^2 = \frac{1}{2}(-b^* - \sqrt{b^{*2} - 4c^*}). \quad (3.14)$$

285 The analysis of the solutions to Eq. (3.13) proceeds with the same procedure presented in Section 2.3;
 286 the details are given in Appendix C.

287 Synthetically, these conclusions can be drawn:

- 288 1. since the discriminant $\Delta^* = b^{*2} - 4c^* > 0$, it results that the squared solutions of biquadratic
 289 equation (3.13), see Eqs. (3.14), are such that $\omega_1^2 \in \mathbb{R}$, $\omega_2^2 \in \mathbb{R}$; moreover, both of them turn out
 290 to be positive;
- 291 2. hence Eq. (3.13) admits four real roots, namely $\pm\sqrt{\omega_1^2}$, $\pm\sqrt{\omega_2^2}$; since negative values of frequency
 292 are physically meaningless, possible vibration modes are identified by either $\omega_n = \sqrt{\omega_1^2}$ or $\omega_n =$
 293 $\sqrt{\omega_2^2}$;
- 294 3. however, in the first part of the spectrum, the frequency of vibration must also comply with
 295 these restrictions:

$$\omega_n < \tilde{\omega} \quad \text{and} \quad \omega_n < \omega_{k_2}^*, \quad (3.15)$$

296 which descends immediately from (B.4), so that the only *admissible solutions* are of the kind:

$$\omega_n = \omega_{k_2} = +\sqrt{\omega_2^2(k_2)}, \quad (k_2 = 1, \dots, k_2^*), \quad (3.16)$$

297 with

$$k_2^* = \max \{k_2 \in \mathbb{N} \mid \omega_{k_2} < \tilde{\omega}\}. \quad (3.17)$$

298 The meaning of Eq. (3.16) is that the k_2 -th frequency is given by the positive root of Eq. (3.14)₂ once
 299 the value $k_2\pi/L$ has been plugged into (3.13).

300 Thus, by virtue of (3.16) the natural frequency for the first part of the spectrum are completely
 301 identified; the definition of the corresponding eigenmodes, $V_n(x) = V_{k_2}(x)$, $\Phi_n(x) = \Phi_{k_2}(x)$ follow
 302 immediately from Eqs. (3.8)–(3.10), taking into account that $A_{1n} = 0$; $A_{3n} = 0$ and considering that,
 303 when $\lambda_2 L = k_2\pi$ it follows from Eqs. (3.12) $\sinh \hat{\lambda}_1 L \neq 0$, which implies $A_{2n} = 0$.

304 Then, by assuming that the eigenfunctions are normalized so that $V_n(x) = V_{k_2}(x)$ has a unit
 305 value when it reaches its absolute maximum, which means $A_{4n} = 1$, one finds:

$$V_{k_2}(x) = \sin \lambda_2 x; \quad \Phi_{k_2}(x) = \frac{\alpha_2}{\lambda_2} \cos \lambda_2 x, \quad (3.18)$$

306 where integer index k_2 belongs to this range:

$$k_2 = 1, \dots, k_2^*. \quad (3.19)$$

307 It has to be emphasized that in Eq. (3.18) $\lambda_2 = \lambda_2(\omega_{k_2})$ and $\alpha_2 = \alpha_2(\omega_{k_2})$ *i.e.* they assume the values
 308 corresponding to ω_{k_2} . The plots of the first eigenmodes which are relevant to the first part of the
 309 spectrum are shown in Figure 2.

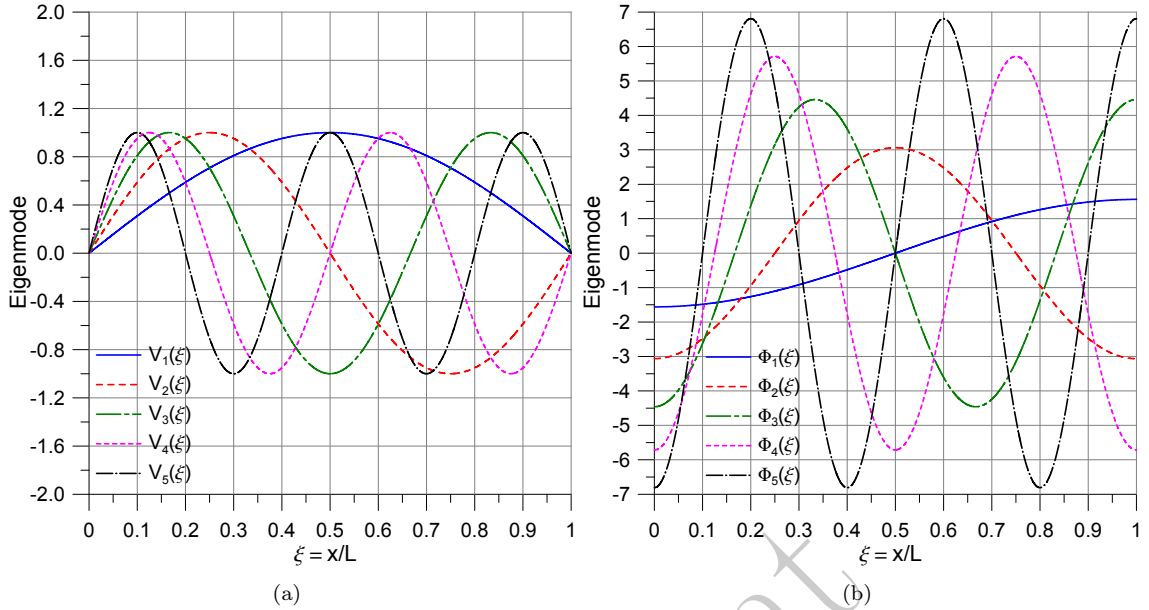


FIGURE 2. Vibration shapes corresponding to modes 1–5 for a simply supported Timoshenko beam, *first* part of the spectrum. (a): transversal displacement, V ; (b): section rotation, Φ . Geometric and material data are given in Section 3.1

310 **3.2.2. Transition frequency:** $\omega^2 = \tilde{\omega}^2$. When BCs are substituted into Eqs. (2.35) and (3.6), a new
 311 homogeneous system of simultaneous linear algebraic equations similar to Eq. (3.8) is obtained; how-
 312 ever, since in this case $\lambda_1^{*2} = 0$, the square matrix \mathbf{A} and the column matrix \mathbf{X} are now given by:
 313

$$\mathbf{A} = \begin{bmatrix} 1 & 1 & 0 & 0 \\ \tilde{\omega}^2 \frac{b}{a} & \tilde{\alpha}_2 & 0 & 0 \\ 1 & \cos \tilde{\lambda}_2 L & \sin \tilde{\lambda}_2 L & 0 \\ \tilde{\omega}^2 \frac{b}{a} & \tilde{\alpha}_2 \cos \tilde{\lambda}_2 L & \tilde{\alpha}_2 \sin \tilde{\lambda}_2 L & 0 \end{bmatrix}, \quad \mathbf{X} = \begin{Bmatrix} C_1 \\ C_3 \\ C_4 \\ D_1 \end{Bmatrix}, \quad (3.20)$$

where, by Eq. (2.30) $\tilde{\lambda}_2 = \sqrt{-\lambda_2^{*2}|_{\omega=\tilde{\omega}}}$, and by Eq. (2.34)

$$\tilde{\alpha}_2 = \tilde{\omega}^2 \frac{b}{a} - \tilde{\lambda}_2^2 = -\frac{a}{c}.$$

314 The coefficient matrix \mathbf{A} appearing in Eq. (3.20) has never $\text{rank}(\mathbf{A}) > 3$. This implies that the
 315 homogeneous system of equations is defective, and this is clearly seen, since it does not depend on
 316 coefficient D_1 .

317 Therefore if the above-mentioned matrix has precisely $\text{rank}(\mathbf{A}) = 3$, *i.e.*, taking advantage of
 318 Eq. (2.34) to simplify the resulting expression:

$$\left(\tilde{\alpha}_2 - \tilde{\omega}^2 \frac{b}{a} \right) \sin \tilde{\lambda}_2 L = -\tilde{\lambda}_2^2 \sin \tilde{\lambda}_2 L \neq 0, \quad (3.21)$$

319 then the only non-trivial solutions to problem (3.8) (when Eq. (3.20) holds) are given by $C_1 = C_{1\tilde{\omega}} = 0$,
 320 $C_3 = C_{3\tilde{\omega}} = 0$, $C_4 = C_{4\tilde{\omega}} = 0$ and $D_1 = D_{1\tilde{\omega}} \neq 0$; in particular the eigenfunction can be normalized
 321 so that $D_{1\tilde{\omega}} = 1$.

322 The eigenfunction for $\omega^2 = \tilde{\omega}^2$ and $\sin \tilde{\lambda}_2 L \neq 0$ is hence:

$$V_{\tilde{\omega}}(x) = 0, \quad \Phi_{\tilde{\omega}}(x) = 1. \quad (3.22)$$

323 The mode described by Eq. (3.22) consists of a *pure-shear* vibration mode (see Figure 3, solid line
 324 plots), where transversal displacement is always zero, while section rotation assumes a constant value,
 325 which is the same for all cross-sections: this ensures that flexural effects do not enter into the play.
 326 Vibrations of Timoshenko beams for this transition frequency, resulting in no transverse deflection,
 have been first studied by Downs, [11].

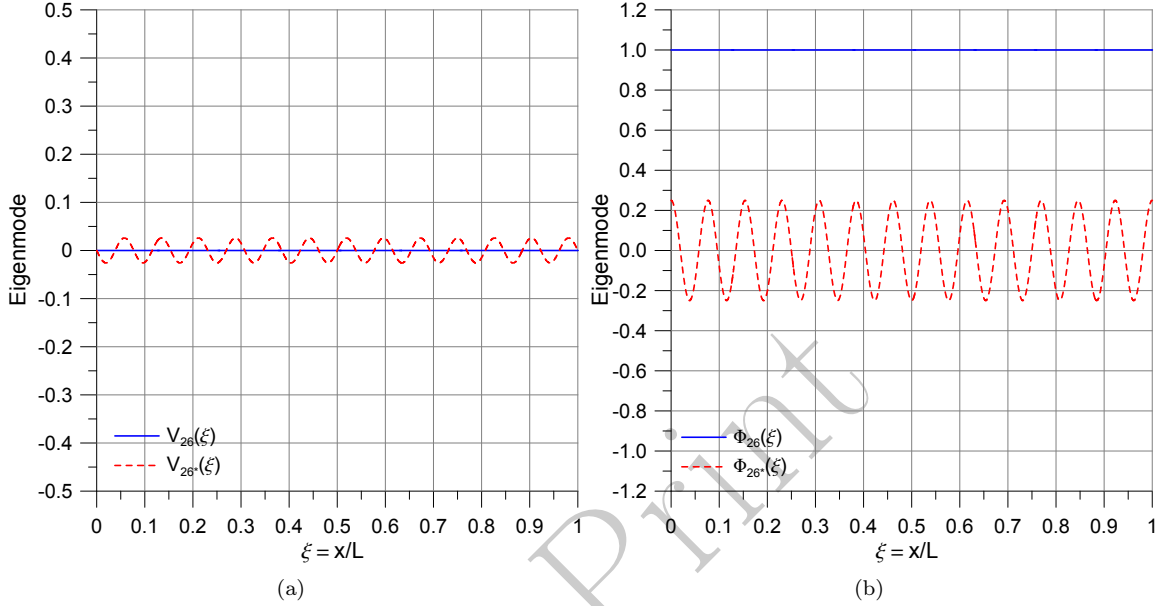


FIGURE 3. Vibration shapes corresponding to the *transition frequency* (mode 26) for a simply supported Timoshenko beam. Transversal displacement, V is shown in (a); section rotation, Φ in (b). The vibration modes for the case of a double eigenmode (which corresponds to a length $\tilde{L} = 2.0519240731$ m) are marked by dashed lines. Geometric and material data are given in Section 3.1.

327 Instead, when the coefficient matrix \mathbf{A} of Eq.(3.20) has $\text{rank}(\mathbf{A}) < 3$, *i.e.* when
 328

$$\tilde{\lambda}_2^2 \sin \tilde{\lambda}_2 L = 0, \quad (3.23)$$

329 this implies that the beam length L has a particular value:

$$L = \tilde{L} = \frac{\tilde{k}\pi}{\tilde{\lambda}_2}, \quad \tilde{k} \in \mathbb{N}, \quad (3.24)$$

330 such that $\sin \tilde{\lambda}_2 \tilde{L} = 0$. Then for $\omega = \tilde{\omega}$ there is a *double eigenvalue*. This condition corresponds to a
 331 length \tilde{L} such that an integer number of sine waves can fit within the beam length, thus satisfying all
 332 BCs; then the space frequency $f_\lambda = f_{\tilde{\lambda}_2} = \tilde{\lambda}_2 \tilde{L} / (2\pi) = \tilde{k} / 2$ turns out to be an integer number (when \tilde{k}
 333 is even) or a half-integer one (when \tilde{k} is odd). As a consequence, non-trivial solutions to problem (3.8)
 334 (when Eq. (3.20) holds) are given by $C_1 = C_{1\tilde{\omega}} = 0$, $C_3 = C_{3\tilde{\omega}} = 0$ while $C_4 = C_{4\tilde{\omega}} \neq 0$ and
 335 $D_1 = D_{1\tilde{\omega}} \neq 0$; in particular the eigenfunction corresponding to the transition frequency depends on
 336 *two arbitrarily chosen* amplitudes $D_{1\tilde{\omega}} = H$, $C_{4\tilde{\omega}} = K$, which correspond to two different eigenmodes.

337 Hence, for the case $\text{rank}(\mathbf{A}) < 3$ (which occurs when $\omega^2 = \tilde{\omega}^2$ and $\sin \tilde{\lambda}_2 L = 0$), the two
 338 eigenfunctions can be written synthetically as:

$$V_{\tilde{\omega}}(x) = K \sin \tilde{\lambda}_2 x, \quad \Phi_{\tilde{\omega}}(x) = H + \frac{\tilde{\alpha}_2}{\tilde{\lambda}_2} K \cos \tilde{\lambda}_2 x. \quad (3.25)$$

339 This is shown again in Figure 3, where the eigenfunctions corresponding to the repeated eigenvalue
 340 are plotted (for the particular choice $K = \tilde{\lambda}_2/(5\tilde{\alpha}_2)$, to improve legibility) with a dashed line.

341 **Remark 4.** The eigenmode corresponding to Eq.(3.22) is *not* a rigid-body mode, since it corresponds
 342 to a frequency value $\omega = \tilde{\omega} \neq 0$ and this shows that to produce a constant cross-section rotation it is
 343 indeed required to have shear strain.

344 On the other hand, the appearance of this pure-shear vibration mode can be prevented by BCs:
 345 so, if both ends of the beam are clamped and not simply-supported this eigenmode does not appear,
 346 and the transition frequency $\tilde{\omega}$ is not, in general, part of the spectrum, unless the beam has a specific
 347 length \tilde{L} . This point will be addressed in [32].

348 **3.2.3. Second part of the spectrum:** $\omega^2 > \tilde{\omega}^2$. In this case, substitution of the BCs into Eqs. (2.37)
 349 and (3.7), gives a homogeneous system of simultaneous linear algebraic equations which is analogous
 350 to Eq. (3.8), but with these definition of the square matrix \mathbf{A} and of the column matrix \mathbf{X} :

$$\mathbf{A} = \begin{bmatrix} 1 & 0 & 1 & 0 \\ \alpha_1 & 0 & \alpha_2 & 0 \\ \cos \lambda_1 L & \sin \lambda_1 L & \cos \lambda_2 L & \sin \lambda_2 L \\ \alpha_1 \cos \lambda_1 L & \alpha_1 \sin \lambda_1 L & \alpha_2 \cos \lambda_2 L & \alpha_2 \sin \lambda_2 L \end{bmatrix}, \quad \mathbf{X} = \begin{Bmatrix} E_1 \\ E_2 \\ E_3 \\ E_4 \end{Bmatrix}. \quad (3.26)$$

351 By taking into account Eqs. (2.22), (2.29)₂ and (2.41), it is an easy task checking that $\alpha_2 - \alpha_1 =$
 352 $\lambda_1^2 - \lambda_2^2 = \lambda_2^{*2} - \lambda_1^{*2} = -\sqrt{\hat{\Delta}} < 0$. It follows from here $E_1 = 0$; $E_3 = 0$ and Eq.(3.8) can be reduced
 353 to:

$$\begin{bmatrix} \sin \lambda_1 L & \sin \lambda_2 L \\ \alpha_1 \sin \lambda_1 L & \alpha_2 \sin \lambda_2 L \end{bmatrix} \begin{Bmatrix} E_2 \\ E_4 \end{Bmatrix} = \begin{Bmatrix} 0 \\ 0 \end{Bmatrix}. \quad (3.27)$$

354 Non-trivial solutions exist provided that $(\alpha_2 - \alpha_1) \sin \lambda_1 L \sin \lambda_2 L = 0$, *i.e.*, being $\alpha_1 - \alpha_2 \neq 0$, when
 355 the following transcendental equation is satisfied:

$$\sin \lambda_1 L \sin \lambda_2 L = 0. \quad (3.28)$$

356 In order to satisfy Eq.(3.28), it must be:

$$\lambda_1 L = k_1 \pi \quad \text{or} \quad \lambda_2 L = k_2 \pi, \quad (k_1, k_2 \in \mathbb{N}). \quad (3.29)$$

The former occurrence implies in this case, for $L \neq 0$, the condition

$$\lambda_1 = k_1 \frac{\pi}{L},$$

357 which can be satisfied by an infinite sequence of integer indices, $k_1 \in \mathbb{N}$. Again, $k_1 = 0$ has to be
 358 discarded since it would give $\lambda_1 = 0$, and that brings back to the transition frequency case, see
 359 Section 3.2.2.

360 In order to find the admissible solutions for λ_1 , it is possible to obtain again the frequency
 361 equation for the simply supported beam, see Eq. (3.13). Details are given in Appendix D.

362 The same discussion of Eq. (3.13) presented in Section 3.2.1 and the findings reported in Appen-
 363 dix C apply here, too, with suitable changes. In particular, these conclusions are outlined:

- 364 1. Eq. (3.13) admits in this case four real roots, namely $\pm\sqrt{\omega_1^2}$, $\pm\sqrt{\omega_2^2}$; if negative values of fre-
 365 quency are disregarded as physically meaningless, possible vibration modes are identified by
 366 either $\omega_n = \sqrt{\omega_1^2}$ or $\omega_n = \sqrt{\omega_2^2}$;
- 367 2. however, in this second part of the spectrum, the frequency of vibration must also comply with
 368 these restrictions:

$$\omega_n > \tilde{\omega} \quad \text{and} \quad \omega_n^2 > \omega_{k_1}^{*2}, \quad (3.30)$$

369 so that only solutions of this kind are *admissible*:

$$\omega_n = \omega_{k_1} = +\sqrt{\omega_1^2(k_1)}, \quad (3.31)$$

370 where the lower bound $\omega_{k_1}^{*2}$ is defined by Eq. (D.3).

371 The notation employed in Eq. (3.31) means that the solution in terms of frequency is given by the
 372 positive root of ω_1^2 , once the value $k_1\pi/L$ has been plugged into it. It has to be noticed that in
 373 Eq. (3.31) the integer index k_1 takes values inside this range:

$$k_1 = 1, \dots, \infty. \tag{3.32}$$

374 By virtue of (3.31) the natural frequency for this first contribution to the second part of the spectrum
 375 are completely identified; the definition of the corresponding eigenmodes, $V_n(x) = V_{k_1}(x)$, $\Phi_n(x) =$
 376 $\Phi_{k_1}(x)$ follows immediately from Eq. (3.8) (when Eq. (3.26) holds), taking into account that $E_{1n} = 0$;
 377 $E_{3n} = 0$ and considering that, when $\lambda_1 L = k_1\pi$ it follows from Eq. (3.27) $E_{4n} = 0$, since $\sin \lambda_2 L \neq 0$.
 378 Then, by assuming a suitable normalization for the eigenfunction, namely $E_{2n} = 1$, one finds:

$$V_{k_1}(x) = \sin \lambda_1 x, \quad \Phi_{k_1}(x) = \frac{\alpha_1}{\lambda_1} \cos \lambda_1 x, \tag{3.33}$$

379 where index k_1 takes the values defined by the range (3.32), while in Eq. (3.33) $\lambda_1 = \lambda_1(\omega_{k_1})$ and
 380 $\alpha_1 = \alpha_1(\omega_{k_1})$, *i.e.* they assume the values corresponding to ω_{k_1} .

381 Some illustrative examples of these eigenmodes are presented in Figure 4; differently from what
 382 happens in Figure 5, here low wave-numbers are encountered, as in the first part of the spectrum: for
 383 comparison purposes, and to outline significant differences, the reader should also look over Figure 2.

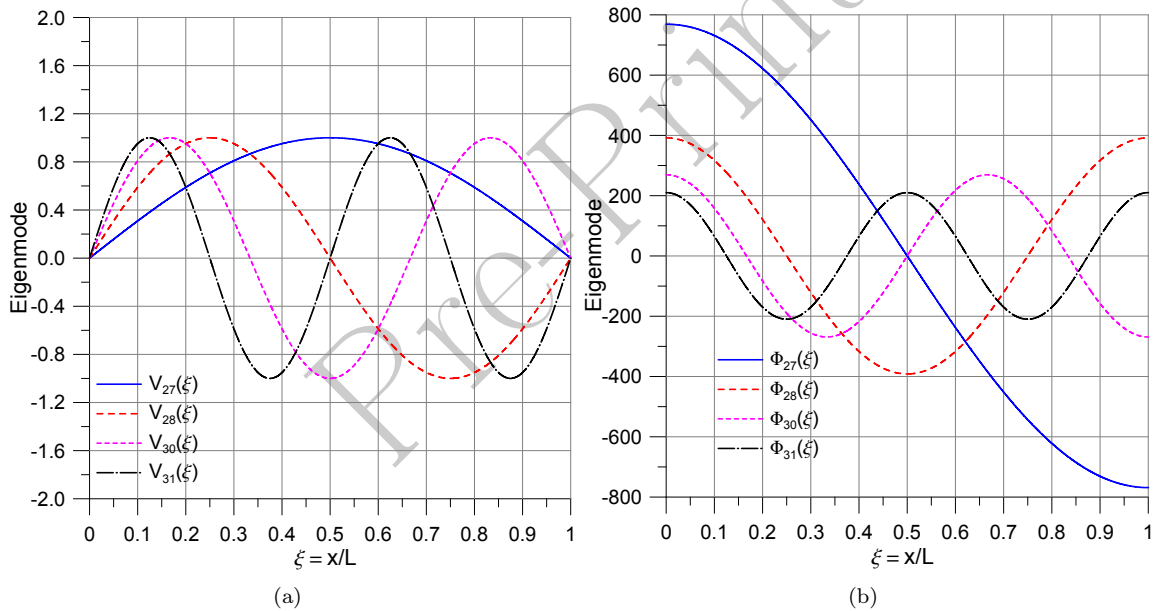


FIGURE 4. Vibration shapes corresponding to λ_1 wave-numbers: modes 27, 28, 30, 31 for a simply supported Timoshenko beam, *second* part of the spectrum. Transversal displacement, V is shown in (a); section rotation, Φ in (b). Geometric and material data are given in Section 3.1.

The latter occurrence (see Eq. (3.29)) gives, for $L \neq 0$:

$$\lambda_2 = k_2 \frac{\pi}{L},$$

384 and provides, see *e.g.* Eq. (B.1) the *same* solution already discussed in Section 3.2.1:

$$\omega_n = \omega_{k_2} = +\sqrt{\omega_2^2(k_2)}, \quad k_2 = k_2^* + 1, \dots, \infty, \tag{3.34}$$

with the only remarkable difference that, being now $\omega > \tilde{\omega}$, index k_2 must take values in a range which extends beyond the value k_2^* which has been defined in Eq. (3.17). On the other hand, the upper bound for $\omega_{k_2}^2$ represented by Eq. (B.4) has still to be satisfied: indeed, if it is violated, no valid solutions are found to Eq. (3.14)₂.

As a consequence, since for $\sin \lambda_2 L$ the solution to problem (3.8) (when Eq. (3.26) holds) is given by $E_{2n} = 0$ and $E_{4n} \neq 0$, if the same normalization is assumed, e.g. $E_{4n} = 1$, the relevant eigenmodes, provided that index k_2 is in the suitable range defined by Eq. (3.34)₂, are:

$$V_{k_2}(x) = \sin \lambda_2 x, \quad \Phi_{k_2}(x) = \frac{\alpha_2}{\lambda_2} \cos \lambda_2 x, \tag{3.35}$$

which still coincide with Eq. (3.18), holding in the first part of the spectrum. It can be checked that this circumstance occurs only in case of a simply supported beam: other combinations of BCs never produce eigenmodes having the same shape in the first and in the second part of the spectrum. Some illustrative examples of these eigenmodes are presented in Figure 5: it should be remarked that they are always associated to *higher* wave-numbers than the corresponding eigenmodes, which are relevant to the first part of the spectrum, see Figure 2.

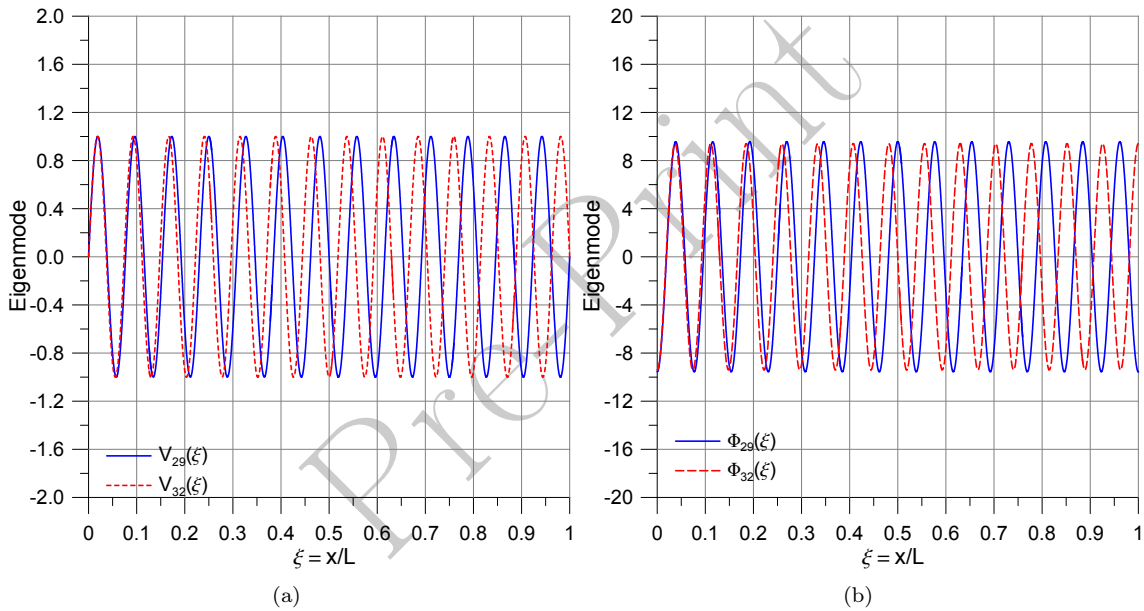


FIGURE 5. Vibration shapes corresponding to λ_2 wave-numbers: modes 29 and 32 for a simply supported Timoshenko beam, *second* part of the spectrum. Transversal displacement, V is shown in (a); section rotation, Φ in (b). Geometric and material data are given in Section 3.1.

3.3. Construction of the spectrum for the simply-supported beam

Having performed the complete analysis for free vibrations of a simply supported Timoshenko beam, it has been acknowledged that the frequency spectrum consists of two parts, separated by a transition frequency,

$$\tilde{\omega} = \sqrt{G\kappa A/(\rho I)},$$

coinciding, as already pointed out in Remark 2, with the cutoff frequency for wave propagation in an infinite Timoshenko beam.

In the first part of the spectrum, frequencies are given by Eq. (3.16), and the corresponding eigenmodes by Eq. (3.18).

In correspondence to the *transition frequency*, $\omega_n = \tilde{\omega}$, which for a simply-supported beam happens to be part of the spectrum, the eigenmode is described by Eq. (3.22) (or by Eq. (3.25), for those particular values of the beam length such that there is a double eigenvalue corresponding to $\tilde{\omega}$).

Finally in the second part of the spectrum there are *two sets* of frequencies, namely:

1. the extension of the previous one, see Eq. (3.34), depending on the λ_2 wave-number, whose eigenmodes are still given by Eq. (3.18);
2. a brand new one, depending on the λ_1 wave-number, which is peculiar of this part of the spectrum, where frequencies are determined by Eq. (3.31) and eigenmodes by Eq. (3.33).

The two sets of frequencies are in this case decoupled, differently from what happens for other combinations of BCs, in the sense that either an eigenmode depends exclusively on the λ_1 wave-number, or it depends solely on the λ_2 one.

In order to proceed to the construction of the spectrum, it is necessary to provide explicitly the material and geometric data of the beam.

Differently from the dynamics of Euler-Bernoulli beam, where the natural frequencies $\omega_{k,EB}$ (and the corresponding eigenmodes $V(x)_{k,EB}$) have very simple expressions for a simply-supported beam:

$$\omega_{k,EB} = (k\pi)^2 \omega^*, \quad \omega^* = \sqrt{\frac{EI}{\rho A}}, \quad V(x)_{k,EB} = \sin\left(\frac{k\pi}{L}x\right), \quad (3.36)$$

and this property allows to build directly the spectrum for the most general case (and in a very general way) as a function of *one dimensionless parameter alone*, ω^* , here such a method cannot be adopted since there are *several independent parameters*.

It is however possible to realize that the transition frequency $\tilde{\omega}$, which allows splitting the spectrum in two parts, depends *only* on the ratio a/d between shear stiffness and rotary inertia and is *independent* of the beam length. Once these parameters are known, it is possible to evaluate it once for all: if the beam length L changes, it is possible to show that $\tilde{\omega}$ *remains fixed*, while the spectrum moves to the right (when L increases) or to the left (if L decreases). For very short beams, it comes out that the transition frequency might correspond to the first mode and the first part of the spectrum vanishes; on the other hand, the longer the beam, the more extended the first part of the spectrum becomes. The second part of the spectrum, however, never vanishes.

Some quantitative results of the transition mode as a function of the length-to-depth ratio L/B for a uniform beam having a square cross-section (having a side length B) at a fixed value of the a/d ratio, see Eq. (2.6), are presented in Table 2 below. In particular, the position of the transition frequency $\tilde{\omega}$ and of the eigenmode corresponding to $k_1 = 1$, Eq. (3.29), within the spectrum, as well as the number of modes (denoted respectively by $N(k_1)$ and $N(k_2)$ corresponding to the λ_1 and the λ_2 wave-numbers are listed there.

Remark 5. A change of vibration modes is peculiar, as it has been shown, of Timoshenko beam theory; however even for the simpler Euler-Bernoulli beam theory a transition between different eigenmodes can occur, for instance, when the beam is partly supported by an elastic foundation. This phenomenon has been thoroughly studied in [47], [48], [49]. Other, more complicated transitions (involving more than one frequency) occur when dealing with modal analysis of plates, either treated by a 2-D elasticity theory [50] or by Reissner-Mindlin theory [51].

3.3.1. Comments on the vibration frequency spectrum. With the above-mentioned data it has been possible to compute the spectrum of natural frequencies for the simply-supported Timoshenko beam up to the first $N = 10,000$ modes; the first $N = 50$ of them have been extracted and are reported in Tables 3–4. The transition frequency occurs in this case for $\tilde{\omega} = 111803.3989$ rad/s, and it happens to be the 26th mode. The interested readers may require to the authors the computer code for computing the natural frequencies for any value of N and for any other geometric and material data.

Looking at the complete list of natural frequencies and at the reduced one (see Tables 3–4), it is interesting to outline these issues:

TABLE 2. Position within the spectrum (corresponding to $N = 10000$ DOFs) of the transition frequency, $n(\tilde{\omega})$, of the first k_1 -eigenmode, $n(k_1 = 1)$, number of k_1 - and k_2 -eigenmodes, for a simply-supported Timoshenko beam having a square cross-section as a function of the length-to-depth ratio L/B for a fixed value of $a/d = 12.5 \cdot 10^9$ (rad/s)²; geometric and material parameters are given in Section 3.1.

L/B	$n(\tilde{\omega})$	$n(k_1 = 1)$	$N(k_1)$	$N(k_2)$
1	2	4	3614	6385
2	3	5	3614	6385
5	7	8	3614	6385
10	13	14	3614	6385
20	26	27	3614	6385
50	64	65	3614	6385
100	127	128	3614	6385
200	254	255	3612	6387
500	634	635	3598	6401
1000	1268	1269	3549	6450

TABLE 3. Computed natural frequencies, wave-numbers and vibration amplitudes of a simply-supported Timoshenko beam for the first $N = 50$ vibration modes: first part of the spectrum and transition frequency. Circular frequency, ω_n is expressed in rad/s, wave-number, λ_n , in rad/m, space frequency, $f_{\lambda_n} = \lambda_n/(2\pi)$ in m⁻¹; all other parameters are dimensionless.

n	k_1	k_2	ω_n	λ_n	f_{λ_n}	$A_{4n} (C_{1n})$	$B_{3n} (D_{1n})$
1	—	1	404.3540829	1.570796327	0.25	1.	-1.560803807
2	—	2	1597.560957	3.141592654	0.50	1.	-3.063603135
3	—	3	3524.348082	4.712388980	0.75	1.	-4.459349847
4	—	4	6104.920320	6.283185307	1.00	1.	-5.713740857
5	—	5	9247.993743	7.853981634	1.25	1.	-6.808596292
6	—	6	1286.193645	9.424777961	1.50	1.	-7.739727835
7	—	7	16862.12383	10.99557429	1.75	1.	-8.513139409
8	—	8	21174.58318	12.56637061	2.00	1.	-9.141129809
9	—	9	25736.94981	14.13716694	2.25	1.	-9.639130208
10	—	10	30497.85749	15.70796327	2.50	1.	-10.02349276
11	—	11	35415.60971	17.27875959	2.75	1.	-10.31011820
12	—	12	40456.65009	18.84955592	3.00	1.	-10.51370482
13	—	13	45594.10054	20.42035225	3.25	1.	-10.64741053
14	—	14	50806.48035	21.99114858	3.50	1.	-10.72276712
15	—	15	56076.63514	23.56194490	3.75	1.	-10.74973665
16	—	16	61390.86478	25.13274123	4.00	1.	-10.73683943
17	—	17	66738.22381	26.70353756	4.25	1.	-10.69131113
18	—	18	72109.96465	28.27433388	4.50	1.	-10.61926501
19	—	19	77499.09604	29.84513021	4.75	1.	-10.52584612
20	—	20	82900.03304	31.41592654	5.00	1.	-10.41537176
21	—	21	88308.31933	32.98672286	5.25	1.	-10.29145567
22	—	22	93720.40640	34.55751919	5.50	1.	-10.15711606
23	—	23	99133.47750	36.12831552	5.75	1.	-10.01486857
24	—	24	104545.3068	37.69911184	6.00	1.	-9.866805432
25	—	25	109954.1463	39.26990817	6.25	1.	-9.714662773
26	—	—	111803.3989	—	—	0.	1.000000000

449 1. For the chosen beam length, the first part of the spectrum encompasses the first 25 natural modes,
 450 all of them corresponding to the λ_2 wave-number (k_2 -eigenmodes) defined by Eq. (3.18). Above
 451 the transition frequencies, where the $\tilde{\omega}$ -eigenmode is given by Eq. (3.22), there appear, irregularly

TABLE 4. Computed natural frequencies, wave-numbers and vibration amplitudes of a simply-supported Timoshenko beam for the first $N = 50$ vibration modes, second part of the spectrum frequency. Circular frequency, ω_n is expressed in rad/s, wave-number, λ_n , in rad/m, space frequency, $f_{\lambda_n} = \lambda_n/(2\pi)$ in m^{-1} ; all other parameters are dimensionless.

n	k_1	k_2	ω_n	λ_n	f_{λ_n}	E_{2n} or E_{4n}	F_{1n} or F_{3n}
27	1	—	112275.2383	1.570796327	0.25	1.	768.8346189
28	2	—	113670.6573	3.141592654	0.50	1.	391.6956430
29	—	26	115358.6353	40.84070450	6.50	1.	-9.559877425
30	3	—	115933.6562	4.712388980	0.75	1.	269.0975234
31	4	—	118983.2427	6.283185307	1.00	1.	210.0200254
32	—	27	120757.7263	42.41150082	6.75	1.	-9.403634895
33	5	—	122726.4860	7.853981634	1.25	1.	176.2477827
34	—	28	126150.6263	43.98229715	7.00	1.	-9.246909765
35	6	—	127069.6867	9.424777961	1.50	1.	155.0442116
36	—	29	131536.7480	45.55309348	7.25	1.	-9.090499676
37	7	—	131925.7658	10.99557429	1.75	1.	140.9585750
38	—	30	136915.6711	47.12388980	7.50	1.	-8.935053917
39	8	—	137217.9485	12.56637061	2.00	1.	131.2748014
40	—	31	142287.1097	48.69468613	7.75	1.	-8.781097464
41	9	—	142880.7632	14.13716694	2.25	1.	124.4925604
42	—	32	147650.8870	50.26548246	8.00	1.	-8.629051189
43	10	—	148859.4765	15.70796327	2.50	1.	119.7187476
44	—	33	153006.9133	51.83627878	8.25	1.	-8.479248853
45	11	—	155108.8098	17.27875959	2.75	1.	116.3905182
46	—	34	158355.1690	53.40707511	8.50	1.	-8.331951400
47	12	—	161591.4548	18.84955592	3.00	1.	114.1367406
48	—	35	163695.6901	54.97787144	8.75	1.	-8.187358974
49	13	—	168276.6548	20.42035225	3.25	1.	112.7034594
50	—	36	169028.5563	56.54866776	9.00	1.	-8.045621043

interspersed with the k_2 -eigenmodes, the natural modes corresponding to the λ_1 wave-number: the k_1 -eigenmodes, which are defined by Eq. (3.33). The first two of them, corresponding to $k_1 = 1$, $k_1 = 2$ occupy positions 27th and 28th in the above-mentioned list.

- For the same values of the k_1 and k_2 indices, the corresponding wave-numbers are equal: this is due to the same form of Eqs. (3.29); however the corresponding natural frequencies ω_{k_1} and ω_{k_2} descend from different solutions of Eq. (3.13) and are therefore different: in particular ω_{k_1} is given by Eq. (3.31), while ω_{k_2} comes out from either Eq. (3.16) or (3.34).
- Looking at the coefficients of the components $\Phi_{k_1}(x)$ and $\Phi_{k_2}(x)$ of the eigenmodes, it results that in all cases $\alpha_1/\lambda_1 > 0$, while $\alpha_2/\lambda_2 < 0$.

This means that in the former case, namely the k_1 -eigenmodes, the *section rotation* $\Phi(x)$ and the *slope of the transversal displacement*, $dV(x)/dx$ have the same sign, *i.e. their contributions to the total shear strain*, see Eq. (2.3)₁, *simply sum up*, while in the latter case, that corresponding to the k_2 -eigenmodes, section rotation and slope of the transversal displacement have opposite sign, so that *the relevant contributions to the total shear strain partly cancel each other*.

Such property had been already detected by Stephen [22, pp. 378–379], even though the explanation which was given there appears rather obscure and unnecessarily complicated.

- For the chosen mechanical and geometric data, when a total number N of natural frequencies is fixed, the composition of the spectrum in terms of k_1 -eigenmodes and k_2 -eigenmodes presents a fairly constant ratio. For instance if $N = 100$ is chosen (*i.e.* the first one hundred natural frequencies are considered), there are 33 k_1 -eigenmodes and 66 k_2 -eigenmodes (plus, of course, the mode corresponding to the *transition frequency* $\tilde{\omega}$); for $N = 500$ the same numbers become

473 180 and 319; similarly, for $N = 1000$ one gets 361 and 638; for $N = 5000$, 1807 and 3192; for
 474 $N = 10000$, 3614 and 6385.

475 For comparison purpose the full spectrum relevant to the first 100 vibration modes for both Euler-
 476 Bernoulli's and the Timoshenko's beam is shown in Figure 6: it is apparent that in the latter case the
 477 vibration frequencies are much less separated than in the former one. This is due to the appearance, in
 the spectrum of Timoshenko beam, of two independent wave-numbers, which are somehow entwined.

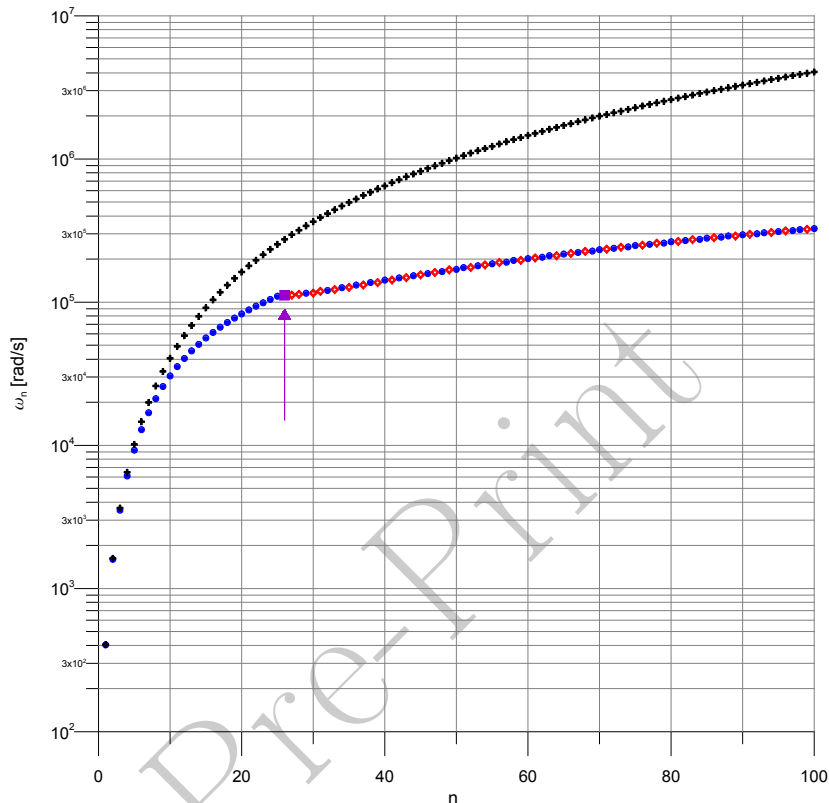


FIGURE 6. Full frequency spectrum, *i.e.* ω_n vs. n plot (for $N=100$ modes) for the simply supported Euler-Bernoulli beam model (denoted by *crosses*) and for the Timoshenko one. For the latter, modes corresponding to λ_2 wave-numbers are marked by solid dots, modes corresponding to λ_1 wave-numbers are denoted by hollow diamonds, while the transition frequency is shown by a solid square: a vertical arrow indicates its position.

478

479 4. Conclusion

480 A complete analysis of the equations of motion for the Timoshenko beam model has been presented in
 481 the case of free vibrations. This has brought to some important results in understanding the nature of
 482 the vibration spectrum, which has often been overlooked in the past. A careful analysis reveals indeed
 483 that there is a transition frequency such that eigenmodes corresponding to natural frequencies lying
 484 below or above it exhibit a rather different shape; moreover, the transition frequency itself might be
 485 part of the spectrum, producing a peculiar vibration mode. As a consequence, the vibration spectrum
 486 of a Timoshenko beam has to be acknowledged to be unique, but consisting of two parts, none of
 487 which can be, in principle, disregarded.

Specific attention has been devoted to the special case of a simply supported beam: the transcendental equation which provides the wave-numbers corresponding to natural frequencies is factorized, and this property produces vibration modes which have in both part of the spectrum (excluding the transition frequency, whose eigenmode is characterized by a constant function) a simple shape, consisting of an integer number of sine/cosine half-waves.

For the given mechanical and geometric data, (which are representative of a beam model where shear strain effects are expected to be non-negligible) a complete list of the first 50 natural frequencies is provided, along with the parameters which are necessary to completely identify the corresponding vibration modes, for both kinematic variables, transversal displacement, V , and cross-section rotation, Φ . The plots of some representative modes are also given, to better illustrate the Timoshenko beam response in terms of free vibrations.

Finally, it is useful to point out that this work provides some useful guidelines to study more complex problems. A first interesting example is the case of curved Timoshenko beams which have been tackled by using the isogeometric approach: in particular, for 1D structures some works have been recently published [52, 53, 54, 55, 56, 57, 58]. Also the use of mixed and hybrid methods and of highly-efficient discretization techniques, such as those reported in [59, 60, 61] are promising. All of them provide more accurate stress description and therefore may improve the relevant numerical results. Geometric nonlinear phenomena and dynamic effects can be explored, too, by using respectively the tools reported in [62, 63, 64, 65, 66, 67, 68] and [69, 70, 71]; for wave propagation problems in second gradient continua and micromorphic materials see also [72, 73, 74, 75, 76].

Furthermore, the Timoshenko beam model, being a particularly simple micro-mechanical model, is able to furnish fruitful clues about developing new and refined mathematical models of continua, see for instance the current research trend on generalized continua and their applications [77, 78, 79, 80, 81, 82, 83, 84, 85, 86, 87, 88, 89], taking also into account the suggestions presented in [90, 91, 92].

Finally, an accurate evaluation of the spectrum is fundamental in problems which consider damage detection, see [93, 94, 95, 96], or which drive the response of smart structures, see [97, 98].

Acknowledgements

The financial support of MIUR, the Italian Ministry of Education, University and Research, under grant PRIN 2010–2011 (project 2010MJBK5B—*Dynamic, Stability and Control of Flexible Structures*) is gratefully acknowledged.

Appendix A. Analysis of the wave-number equation

To investigate the nature of the eigensolutions, it is essential to check whether the roots of the bi-quadratic Eq. (2.19) are either real or complex conjugates. In particular, the following steps have to be performed.

1. identifying the sign of the discriminant $\hat{\Delta} = \hat{b}^2 - 4\hat{c}$;
2. verifying whether $\lambda_2^{*2} > 0$ or $\lambda_2^{*2} = 0$ or $\lambda_2^{*2} < 0$;
3. verifying whether $\lambda_1^{*2} > 0$ or $\lambda_1^{*2} = 0$ or $\lambda_1^{*2} < 0$.

Preliminarily, it can be stated that all material properties, as well as cross-section data, have to be positive for physical reasons. Now the above-mentioned tasks will be accomplished in the afore-listed order.

1. First, attention is concentrated on the sign of the discriminant. Then, account taken of Eqs. (2.20)–(2.21), it is possible to show that:

$$\hat{\Delta} = \frac{\rho^2 \omega^4}{E^2} \left(1 + \frac{E}{G\kappa} \right)^2 - 4 \frac{\rho^2 \omega^4}{E^2} \frac{E}{G\kappa} + 4 \frac{\rho \omega^2 A}{EI} = \frac{\rho^2 \omega^4}{E^2} \left(1 - \frac{E}{G\kappa} \right)^2 + 4 \frac{\rho \omega^2 A}{EI} > 0. \quad (\text{A.1})$$

So the discriminant $\hat{\Delta}$, being the sum of positive quantities, never becomes negative.

531 Moreover $\hat{\Delta} = 0$ implies either $\omega^2 = 0$ or

$$\omega^2 = -\frac{\frac{4EA}{\rho I}}{\left(1 - \frac{E}{G\kappa}\right)^2} < 0. \quad (\text{A.2})$$

532 Hence $\hat{\Delta}$ vanishes only for *one value* of $\omega \in \mathbb{R}$, namely $\omega = 0$.

533 It follows from here that the two roots λ_1^{*2} , λ_2^{*2} defined by Eq. (2.22) do coincide only when
534 $\omega = 0$. For such value, it is simply:

$$\lambda_1^{*2} = \lambda_2^{*2} = -\frac{\hat{b}}{2}\Big|_{\omega=0} = 0. \quad (\text{A.3})$$

535 2. As a consequence, since the sum of two negative quantities cannot be positive, it follows that
536 $\lambda_2^{*2} \leq 0$, and $\lambda_2^{*2} = 0$ *only when* $\omega = 0$; in all other instances it is strictly $\lambda_2^{*2} < 0$.

537 3. Finally, it is required investigating the sign of λ_1^{*2} . By substitution, it can be written in this
538 equivalent form:

$$\lambda_1^{*2} = -\frac{\rho\omega^2}{2E} \left(1 + \frac{E}{G\kappa}\right) + \sqrt{\frac{\rho^2\omega^4}{4E^2} \left(1 - \frac{E}{G\kappa}\right)^2 + \frac{\rho\omega^2 A}{EI}}. \quad (\text{A.4})$$

539 It is now an easy task checking that:

$$\lambda_1^{*2} > 0 \Rightarrow \sqrt{\frac{\rho^2\omega^4}{4E^2} \left(1 - \frac{E}{G\kappa}\right)^2 + \frac{\rho\omega^2 A}{EI}} > \frac{\rho\omega^2}{2E} \left(1 + \frac{E}{G\kappa}\right), \quad (\text{A.5})$$

and since both the r.h.s. and the l.h.s. of expression (A.5) are strictly positive, inequality is preserved if they are squared. Thus, after canceling common terms on both sides of the inequality it follows that:

$$\frac{A}{I} > \frac{\rho\omega^2}{G\kappa} \Rightarrow \omega^2 < \frac{G\kappa A}{\rho I} = \tilde{\omega}^2.$$

Hence the conclusion for item 3. above is:

$$\begin{aligned} \lambda_1^{*2} &> 0 && \text{if } \omega^2 < \tilde{\omega}^2, \\ \lambda_1^{*2} &= 0 && \text{if } \omega^2 = \tilde{\omega}^2, \\ \lambda_1^{*2} &< 0 && \text{if } \omega^2 > \tilde{\omega}^2. \end{aligned} \quad (\text{A.6})$$

540 In conclusion, according to the value assumed by ω^2 with reference to $\tilde{\omega}^2$, three different cases have
541 to be distinguished.

542 Appendix B. Deduction of the frequency equation for the simply supported beam

543 By Eqs. (2.20), (2.21), (2.22)₂ and (3.12)₂ this equivalent expression for ω is obtained:

$$\sqrt{\frac{\rho^2\omega^4}{4E^2} \left(1 - \frac{E}{G\kappa}\right)^2 + \frac{\rho\omega^2 A}{EI}} = \left(\frac{k_2\pi}{L}\right)^2 - \frac{\rho\omega^2}{2E} \left(1 + \frac{E}{G\kappa}\right). \quad (\text{B.1})$$

The right- and left-hand sides of this equation can be squared, giving an equivalent expression, *only if they have the same sign, i.e.* provided that:

$$\left(\frac{k_2\pi}{L}\right)^2 - \frac{\rho\omega^2}{E} \left(1 + \frac{E}{G\kappa}\right) > 0,$$

544 and the result is:

$$\frac{\rho}{2E} \left(1 + \frac{E}{G\kappa}\right) \omega^2 < \left(\frac{k_2\pi}{L}\right)^2. \quad (\text{B.2})$$

545 Since, by Eq. (2.6), the factor multiplying ω^2 in Eq. (B.2) can be given this form:

$$D = \frac{1}{2} \frac{\rho}{E} \left(1 + \frac{E}{G\kappa} \right) = \frac{1}{2} \left(\frac{d}{c} + \frac{b}{a} \right), \quad (\text{B.3})$$

546 where $D > 0$ is a constant, independent of k_2 , it follows that Eq. (B.2) is equivalent to imposing this
547 upper bound on the value of ω^2 corresponding to a given value of index k_2 :

$$\omega^2 < \frac{1}{D} \left(\frac{k_2\pi}{L} \right)^2 = \omega_{k_2}^*{}^2. \quad (\text{B.4})$$

548 In particular, Eq. (B.4) requires eliminating $k_2 = 0$ from the set of admissible values, since it would
549 give a negative value for ω^2 .

550 By squaring both sides of Eq. (B.1) and after some rearrangements, the following result is ob-
551 tained:

$$\omega^4 - \frac{G\kappa}{\rho} \left[\frac{A}{I} + \left(\frac{k_2\pi}{L} \right)^2 \left(1 + \frac{E}{G\kappa} \right) \right] \omega^2 + \frac{EG\kappa}{\rho^2} \left(\frac{k_2\pi}{L} \right)^4 = 0. \quad (\text{B.5})$$

552 A final compact form of Eq. (B.5) is arrived at, if the following short-hand notation is adopted:

$$b^* = -\frac{G\kappa}{\rho} \left[\frac{A}{I} + \left(\frac{k_2\pi}{L} \right)^2 \left(1 + \frac{E}{G\kappa} \right) \right], \quad c^* = \frac{EG\kappa}{\rho^2} \left(\frac{k_2\pi}{L} \right)^4, \quad (\text{B.6})$$

producing as a result the biquadratic equation:

$$\omega^4 + b^*\omega^2 + c^* = 0.$$

553 Appendix C. Analysis of the frequency equation

554 The same procedure presented in Appendix A is here used for investigating the solutions, Eq. (3.14),
555 of the frequency equation for the simply-supported beam, Eq. (3.13):

- 556 1. The sign of the discriminant $\Delta^* = b^{*2} - 4c^*$;
- 557 2. For which values of the parameters $\omega_1^2 > 0$ and satisfies the requirement expressed by Eq. (B.2);
- 558 3. For which values of the parameters $\omega_2^2 > 0$ and satisfies the requirement expressed by Eq. (B.2).

559 The analysis proceeds as follows:

1. It can be easily verified that Δ^* might be written equivalently as:

$$\Delta^* = \left(\frac{G\kappa}{\rho} \right)^2 \left[\left(\frac{A}{I} \right)^2 + 2 \frac{A}{I} \left(1 + \frac{E}{G\kappa} \right) \left(\frac{k\pi}{L} \right)^2 + \left(1 - \frac{E}{G\kappa} \right)^2 \left(\frac{k\pi}{L} \right)^4 \right].$$

560 Now, $\Delta^* > 0$, since it comes out to be the sum of positive values only.

- 561 2. Since $\Delta^* > 0$ it is also true, by virtue of Eq. (3.14)₁, (B.6), that $\omega_1^2 > 0$ for all possible values
562 of the parameters.

However, with reference to the requirement expressed by Eq. (B.2) it can be shown, after some lengthy computations, that it is equivalent to imposing:

$$\frac{G\kappa}{4E} \left[\left(1 + \frac{E}{G\kappa} \right) \frac{A}{I} + \left(1 - \frac{E}{G\kappa} \right)^2 \left(\frac{k_2\pi}{L} \right)^2 \right] + \frac{\rho}{4E} \left(1 + \frac{E}{G\kappa} \right) \sqrt{\Delta^*} < 0,$$

563 which is impossible, since the sum of addends which are always positive never produces a negative
564 number. Hence the value $\omega_1^2 > 0$ is not admissible in the present case.

3. The condition $\omega_2^2 > 0$ requires that $-b^* > \Delta^*$ and can be stated in this equivalent form:

$$\left[\frac{A}{I} + \left(1 + \frac{E}{G\kappa} \right) \left(\frac{k_2\pi}{L} \right)^2 \right] > \sqrt{\left[\left(\frac{A}{I} \right)^2 + 2 \frac{A}{I} \left(1 + \frac{E}{G\kappa} \right) \left(\frac{k_2\pi}{L} \right)^2 + \left(1 - \frac{E}{G\kappa} \right)^2 \left(\frac{k_2\pi}{L} \right)^4 \right]}$$

and after some algebraic manipulation it can be reduced to the condition:

$$\left(1 + \frac{E}{G\kappa}\right)^2 > \left(1 - \frac{E}{G\kappa}\right)^2,$$

565 which is always satisfied.

Moreover, the frequency value given by ω_2^2 is *fully admissible*, since it can be shown to satisfy also the requirement given by Eq. (B.2). Indeed, after some cumbersome algebra it turns out:

$$\left[2\frac{A}{I}\left(\frac{k_2\pi}{L}\right)^2\left(1 + \frac{E}{G\kappa}\right)^2 + \left(\frac{k_2\pi}{L}\right)^4\left(1 - \frac{E}{G\kappa}\right)^2\right] \left[\left(1 - \frac{E}{G\kappa}\right)^2 - \left(1 + \frac{E}{G\kappa}\right)^2\right] < 0,$$

566 which is always satisfied, since the last term within square brackets is always negative.

567 Appendix D. The frequency equation for the simply supported beam in the second 568 part of the spectrum

569 It is necessary to recall that, by substituting (2.20), (2.21), (2.22)₁ and (3.29)₁ this equivalent expres-
570 sion for ω is found:

$$\sqrt{\frac{\rho^2\omega^4}{4E^2}\left(1 - \frac{E}{G\kappa}\right)^2 + \frac{\rho\omega^2 A}{EI}} = \frac{\rho\omega^2}{2E}\left(1 + \frac{E}{G\kappa}\right) - \left(\frac{k_1\pi}{L}\right)^2. \quad (\text{D.1})$$

The r.h.s. and l.h.s of this equation can be squared, as usual, only if they have the same sign:

$$\frac{\rho\omega^2}{E}\left(1 + \frac{E}{G\kappa}\right) - \left(\frac{k_1\pi}{L}\right)^2 > 0,$$

571 and the result is:

$$\frac{\rho}{2E}\left(1 + \frac{E}{G\kappa}\right)\omega^2 > \left(\frac{k_1\pi}{L}\right)^2. \quad (\text{D.2})$$

572 If Eq. (B.3) is recalled, the following lower bound for ω^2 as a function of index k_1 is established:

$$\omega^2 > \frac{1}{D}\left(\frac{k_1\pi}{L}\right)^2 = \omega_{k_1}^*{}^2. \quad (\text{D.3})$$

573 By squaring both sides of Eq. (D.1) and after performing some rearrangements, the same *fre-*
574 *quency equation* for the simply-supported Timoshenko beam is obtained:

$$\omega^4 - \frac{G\kappa}{\rho}\left[\frac{A}{I} + \left(\frac{k_1\pi}{L}\right)^2\left(1 + \frac{E}{G\kappa}\right)\right]\omega^2 + \frac{EG\kappa}{\rho^2}\left(\frac{k_1\pi}{L}\right)^4 = 0, \quad (\text{D.4})$$

575 see Eq. (B.5), with the simple substitution of k_1 in the position previously hold by k_2 . Clearly, in this
576 case, admissible solutions for ω_1^2 must comply with the requirement expressed by Eq. (D.3).

577 References

- 578 [1] S.P. Timoshenko. On the correction for shear of the differential equation for transverse vibrations
579 of prismatic bars. *Philosophical Magazine (Series 5)*, 41:744–746, 1921.
- 580 [2] S.P. Timoshenko. On the transverse vibrations of bars of uniform cross-section. *Philosophical*
581 *Magazine (Series 5)*, 43:125–131, 1922.
- 582 [3] J. Stefan. *Über die Transversalschwingungen eines elastischen Stabes*. K.K. Hof- und Staats-
583 druckerei, Wien, 1858.
- 584 [4] J.W. Strutt (Baron Rayleigh). *The Theory of Sound*, volume 1. Macmillan and Co., London,
585 1877.
- 586 [5] S.M. Han, H. Benaroya, and T. Wei. Dynamics of transversely vibrating beams using four
587 engineering theories. *Journal of Sound and Vibration*, 225:935–988, 1999.

- 588 [6] A. Labuschagne, N.F.J. van Rensburg, and A.J. van der Merwe. Comparison of linear beam
589 theories. *Mathematical and Computer Modelling*, 49:20–30, 2009.
- 590 [7] B.H. Karnopp. Duality relations in the analysis of beam oscillations. *Zeitschrift für Angewandte*
591 *Mathematik und Physik (ZAMP)*, 18:575–580, 1967.
- 592 [8] B. Tabarrok and B.H. Karnopp. Analysis of the oscillations of the Timoshenko beam. *Zeitschrift*
593 *für Angewandte Mathematik und Physik (ZAMP)*, 18:580–587, 1967.
- 594 [9] J.G. Easley. Nonlinear vibration of beams and rectangular plates. *Zeitschrift für Angewandte*
595 *Mathematik und Physik (ZAMP)*, 15:167–175, 1964.
- 596 [10] R. W. Traill-Nash and A. R. Collar. The effects of shear flexibility and rotatory inertia on the
597 bending vibrations of beams. *The Quarterly Journal of Mechanics and Applied Mathematics*,
598 6:186–222, 1953.
- 599 [11] B. Downs. Transverse vibration of a uniform, simply supported Timoshenko beam without trans-
600 verse deflection. *Journal of Applied Mechanics*, 43:671–674, 1976.
- 601 [12] B.A.H. Abbas and J. Thomas. The second frequency spectrum of Timoshenko beams. *Journal*
602 *of Sound and Vibration*, 51:123–137, 1977.
- 603 [13] G.R. Bhashyam and G. Prathap. The second frequency spectrum of Timoshenko beams. *Journal*
604 *of Sound and Vibration*, 76:407–420, 1981.
- 605 [14] M. Levinson and D.W. Cooke. On the two frequency spectra of Timoshenko beams. *Journal of*
606 *Sound and Vibration*, 84:319–326, 1982.
- 607 [15] N.G. Stephen. The second frequency spectrum of Timoshenko beams. *Journal of Sound and*
608 *Vibration*, 80:578–582, 1982.
- 609 [16] G. Prathap. The two frequency spectra of timoshenko beams — A re-assessment. *Journal of*
610 *Sound and Vibration*, 90:443–445, 1983.
- 611 [17] M. Levinson. Author’s reply. *Journal of Sound and Vibration*, 90:445–446, 1983.
- 612 [18] V.V. Nesterenko. A theory for transverse vibrations of the Timoshenko beam. *PMM-Journal of*
613 *Applied Mathematics and Mechanics*, 57:669–677, 1993.
- 614 [19] V.V. Nesterenko and A.M. Chervyakov. Parabolic approximation to the theory of transverse
615 vibrations of rods and beams. *Journal of Applied Mechanics and Technical Physics*, 35:306–309,
616 1994.
- 617 [20] P. Olsson and G. Kristensson. Wave splitting of the Timoshenko beam equation in the time
618 domain. *Zeitschrift für Angewandte Mathematik und Physik (ZAMP)*, 45:866–881, 1994.
- 619 [21] S. Ekwaro-Osire, D.H.S. Maithripala, and J.M. Berg. A series expansion approach to interpreting
620 the spectra of the Timoshenko beam. *Journal of Sound and Vibration*, 240:667–678, 2001.
- 621 [22] N.G. Stephen. The second spectrum of Timoshenko beam theory — Further assessment. *Journal*
622 *of Sound and Vibration*, 292:372–389, 2006.
- 623 [23] N.G. Stephen and S. Puchegger. On the valid frequency range of Timoshenko beam theory.
624 *Journal of Sound and Vibration*, 297:1082–1087, 2006.
- 625 [24] A. Bhaskar. Elastic waves in Timoshenko beams: the ‘lost and found’ of an eigenmode. *Proceedings*
626 *of the Royal Society/A: Mathematical Physical & Engineering Sciences*, 465:239–255, 2009.
- 627 [25] I. Senjanović and N. Vladimir. Physical insight into Timoshenko beam theory and its modification
628 with extension. *Structural Engineering and Mechanics*, 48(4):519–545, 2013.
- 629 [26] N.F.J. van Rensburg and A.J. van der Merwe. Natural frequencies and modes of a Timoshenko
630 beam. *Wave Motion*, 44:58–69, 2006.
- 631 [27] W.D. Pilkey. *Formulas for stress, strain, and structural matrices*. Wiley, Hoboken, NJ, 2nd
632 edition, 2005.
- 633 [28] J.N. Reddy. *Mechanics of laminated composite plates and shells: theory and analysis*. CRC Press,
634 Boca Raton, FL, 2ed. edition, 2003.
- 635 [29] I.A. Karnowsky and O.I. Lebed. *Formulas for structural dynamics — Tables, graphs and solutions*.
636 McGraw-Hill, New York, 2001.
- 637 [30] A. Cazzani, F. Stochino, and E. Turco. A computational assessment via finite elements and
638 isogeometric analysis of the whole spectrum of Timoshenko beams. *submitted*, pages 1–25, 2015.

- 639 [31] K.F. Graff. *Wave motion in elastic solids*. Oxford University Press, London, 1975.
- 640 [32] A. Cazzani, F. Stochino, and E. Turco. On the whole spectrum of Timoshenko beams. Part II:
641 further applications. *submitted*, pages 1–22, 2015.
- 642 [33] E. Goens. Über die Bestimmung des Elastizitätsmoduls von Stäben mit Hilfe von Biegungss-
643 chwingungen. *Annalen der Physik (Series 5)*, 403:649–678, 1931.
- 644 [34] A. Föppl. *Vorlesungen über technische Mechanik — Dritter Band: Festigkeitslehre*. B.G. Teubner,
645 Leipzig, 1897.
- 646 [35] T. Kaneko. On Timoshenko’s correction for shear in vibrating beams. *Journal of Physics/D:
647 Applied Physics*, 8:1927–1936, 1975.
- 648 [36] J.J. Jensen. On the shear coefficient in Timoshenko’s beam theory. *Journal of Sound and
649 Vibration*, 87:621–635, 1983.
- 650 [37] J.D. Renton. A note on the form of the shear coefficient. *International Journal of Solids and
651 Structures*, 34:1681–1685, 1997.
- 652 [38] R.A. Méndez-Sánchez, A. Morales, and J. Flores. Experimental check on the accuracy of Timo-
653 shenko’s beam theory. *Journal of Sound and Vibration*, 279:508–512, 2005.
- 654 [39] S.B. Dong, C. Alpdogan, and E. Taciroglu. Much ado about shear correction factors in Timo-
655 shenko beam theory. *International Journal of Solids and Structures*, 47:1651–1665, 2010.
- 656 [40] G.R. Cowper. The shear coefficient in Timoshenko’s beam theory. *Journal of Applied Mechanics*,
657 33:335–340, 1966.
- 658 [41] S. Higuchi, H. Saito, and C. Hashimoto. A study of the approximate theory of an elastic thick
659 beam. *Canadian Journal of Physics*, 35(6):757–765, 1957.
- 660 [42] J. R. Hutchinson. Shear coefficients for Timoshenko beam theory. *Journal of Applied Mechanics*,
661 68:87–92, 2001.
- 662 [43] N.G. Stephen. On the variation of Timoshenko’s shear coefficient with frequency. *Journal of
663 Applied Mechanics*, 45:695–697, 1978.
- 664 [44] N.G. Stephen. On “A check on the accuracy of Timoshenko’s beam theory”. *Journal of Sound
665 and Vibration*, 257:809–812, 2002.
- 666 [45] K.T. Chan, K.F. Lai, N.G. Stephen, and K. Young. A new method to determine the shear
667 coefficient of Timoshenko beam theory. *Journal of Sound and Vibration*, 330:3488–3497, 2011.
- 668 [46] H. E. Rosinger and I. G. Ritchie. On Timoshenko’s correction for shear in vibrating isotropic
669 beams. *Journal of Physics/D: Applied Physics*, 10:1461–1466, 08 1977.
- 670 [47] P.F. Doyle and M.N. Pavlovic. Vibration of beams on partial elastic foundations. *Earthquake
671 Engineering and Structural Dynamics*, 10:663–674, 1982.
- 672 [48] M. Eisenberger, D.Z. Yankelevsky, and M.A. Adin. Vibrations of beams fully or partially sup-
673 ported on elastic foundations. *Earthquake Engineering and Structural Dynamics*, 13:651–660,
674 1985.
- 675 [49] A. Cazzani. On the dynamics of a beam partially supported by an elastic foundation: An exact
676 solution-set. *International Journal of Structural Stability and Dynamics*, 13:1350045/1–30, 2013.
677 DOI:10.1142/S0219455413500454.
- 678 [50] M. Levinson. Free vibrations of a simply supported, rectangular plate: An exact elasticity solution.
679 *Journal of Sound and Vibration*, 98:289–298, 1985.
- 680 [51] N.G. Stephen. Mindlin plate theory: Best shear coefficient and higher spectra validity. *Journal
681 of Sound and Vibration*, 202:539–553, 1997.
- 682 [52] A. Cazzani, M. Malagù, and E. Turco. Isogeometric analysis of plane-curved beams. *Mathematics
683 and Mechanics of Solids*, pages 1–16, 2014. DOI:10.1177/1081286514531265.
- 684 [53] A. Cazzani, M. Malagù, and E. Turco. Isogeometric analysis: a powerful numerical tool for the
685 elastic analysis of historical masonry arches. *Continuum Mechanics and Thermodynamics*, pages
686 1–18, 2014. DOI:10.1007/s00161-014-0409-y.
- 687 [54] A. Cazzani, M. Malagù, E. Turco, and F. Stochino. Constitutive models for strongly curved
688 beams in the frame of isogeometric analysis. *Mathematics and Mechanics of Solids*, pages 1–28,
689 2015. DOI:10.1177/1081286515577043.

- 690 [55] A. Chiozzi, M. Malagù, A. Tralli, and A. Cazzani. ArchNURBS: NURBS-based tool for the
691 structural safety assessment of masonry arches in MATLAB. *Journal of Computing in Civil*
692 *Engineering*, pages 1–11, 2015. DOI:10.1061/(ASCE)CP.1943-5487.0000481.
- 693 [56] M. Cuomo, L. Contrafatto, and L. Greco. A variational model based on isogeometric interpolation
694 for the analysis of cracked bodies. *International Journal of Engineering Science*, 80:173–188, 2014.
- 695 [57] L. Greco and M. Cuomo. An implicit G^1 multi patch B-spline interpolation for Kirchhoff-Love
696 space rod. *Computer Methods in Applied Mechanics and Engineering*, 269:173–197, 2014.
- 697 [58] L. Greco and M. Cuomo. B-Spline interpolation of Kirchhoff-Love space rods. *Computer Methods*
698 *in Applied Mechanics and Engineering*, 256:251–269, 2013.
- 699 [59] A. Cazzani, E. Garusi, A. Tralli, and S.N. Atluri. A four-node hybrid assumed-strain finite
700 element for laminated composite plates. *Computers, Materials & Continua*, 2:23–38, 2005.
- 701 [60] A. Bilotta, G. Formica, and E. Turco. Performance of a high-continuity finite element in three-
702 dimensional elasticity. *International Journal for Numerical Methods in Biomedical Engineering*
703 *(Communications in Numerical Methods in Engineering)*, 26:1155–1175, 2010.
- 704 [61] E. Turco and P. Caracciolo. Elasto-plastic analysis of Kirchhoff plates by high simplicity finite
705 elements. *Computer Methods in Applied Mechanics and Engineering*, 190:691–706, 2000.
- 706 [62] N. Rizzi, V. Varano, and S. Gabriele. Initial postbuckling behavior of thin-walled frames under
707 mode interaction. *Thin-Walled Structures*, 68:124–134, 2013.
- 708 [63] S. Gabriele, N. Rizzi, and V. Varano. A 1D higher gradient model derived from Koiter’s shell
709 theory. *Mathematics and Mechanics of Solids*, pages 1–10, 2014. DOI: 10.1177/1081286514536721.
- 710 [64] N. Rizzi and V. Varano. The effects of warping on the postbuckling behaviour of thin-walled
711 structures. *Thin-Walled Structures*, 49(9):1091–1097, 2011.
- 712 [65] D. Zulli and A. Luongo. Bifurcation and stability of a two-tower system under wind-induced
713 parametric, external and self-excitation. *Journal of Sound and Vibration*, 331(2):365 – 383, 2012.
- 714 [66] M. Pignataro, N. Rizzi, G. Ruta, and V. Varano. The effects of warping constraints on the
715 buckling of thin-walled structures. *Journal of Mechanics of Material and Structures*, 4(10):1711–
716 1727, 2009.
- 717 [67] G.C. Ruta, V. Varano, M. Pignataro, and N.L. Rizzi. A beam model for the flexural-torsional
718 buckling of thin-walled members with some applications. *Thin-Walled Structures*, 46(7–9):816 –
719 822, 2008.
- 720 [68] F. Presta, C.R. Hendy, and E. Turco. Numerical validation of simplified theories for design rules
721 of transversely stiffened plate girders. *The Structural Engineer*, 86(21):37–46, 2008.
- 722 [69] G. Piccardo, G. Ranzi, and A. Luongo. A complete dynamic approach to the generalized beam
723 theory cross-section analysis including extension and shear modes. *Mathematics and Mechanics*
724 *of Solids*, 19(8):900–924, 2014.
- 725 [70] G. Piccardo, F. Tubino, and A. Luongo. Equivalent nonlinear beam model for the 3-D analysis of
726 shear-type buildings: Application to aeroelastic instability. *International Journal of Non-Linear*
727 *Mechanics*, 2015. DOI:10.1016/j.ijnonlinmec.2015.07.013.
- 728 [71] D. Del Vescovo and I. Giorgio. Dynamic problems for metamaterials: review of existing models
729 and ideas for further research. *International Journal of Engineering Science*, 80:153–172, 2014.
- 730 [72] F. dell’Isola, A. Madeo, and L. Placidi. Linear plane wave propagation and normal transmission
731 and reflection at discontinuity surfaces in second gradient 3D continua. *ZAMM - Journal of*
732 *Applied Mathematics and Mechanics / Zeitschrift für Angewandte Mathematik und Mechanik*,
733 92(1):52–71, 2012.
- 734 [73] A. Berezovski, I. Giorgio, and A. Della Corte. Interfaces in micromorphic materials: Wave trans-
735 mission and reflection with numerical simulations. *Mathematics and Mechanics of Solids*, 2015.
736 DOI: 10.1177/1081286515572244.
- 737 [74] A. Madeo, P. Neff, I.-D. Ghiba, L. Placidi, and G. Rosi. Band gaps in the relaxed linear micro-
738 morphic continuum. *ZAMM - Journal of Applied Mathematics and Mechanics / Zeitschrift für*
739 *Angewandte Mathematik und Mechanik*, 95(9):880–887, 2015.

- [75] A. Madeo, P. Neff, I.D. Ghiba, L. Placidi, and G. Rosi. Wave propagation in relaxed micromorphic continua: modeling metamaterials with frequency band-gaps. *Continuum Mechanics and Thermodynamics*, 27(4-5):551–570, 2015.
- [76] L. Placidi, G. Rosi, I. Giorgio, and A. Madeo. Reflection and transmission of plane waves at surfaces carrying material properties and embedded in second-gradient materials. *Mathematics and Mechanics of Solids*, 2013. DOI: 10.1177/1081286512474016.
- [77] F. dell’Isola, T. Lekszycki, M. Pawlikowski, R. Grygoruk, and L. Greco. Designing a light fabric metamaterial being highly macroscopically tough under directional extension: first experimental evidence. *Zeitschrift für Angewandte Mathematik und Physik (ZAMP)*, pages 1–26, 2015. DOI:10.1007/s00033-015-0556-4.
- [78] U. Andreaus, I. Giorgio, and A. Madeo. Modeling of the interaction between bone tissue and resorbable biomaterial as linear elastic materials with voids. *Zeitschrift für Angewandte Mathematik und Physik (ZAMP)*, 66(1):209–237, 2015.
- [79] A. Grillo, S. Federico, and G. Wittum. Growth, mass transfer, and remodeling in fiber-reinforced, multi-constituent materials. *International Journal of Non-Linear Mechanics*, 47(2):388–401, 2012.
- [80] S. Federico, A. Grillo, S. Imatani, G. Giacquinta, and W. Herzog. An energetic approach to the analysis of anisotropic hyperelastic materials. *International Journal of Engineering Science*, 46:164–181, 2008.
- [81] J.-J. Alibert and A. Della Corte. Second-gradient continua as homogenized limit of pantographic microstructured plates: a rigorous proof. *Zeitschrift für Angewandte Mathematik und Physik (ZAMP)*, 66:2855–2870, 2015.
- [82] F. dell’Isola, U. Andreaus, and L. Placidi. At the origins and in the vanguard of peridynamics, non-local and higher-gradient continuum mechanics: An underestimated and still topical contribution of Gabrio Piola. *Mathematics and Mechanics of Solids*, 20(8):887–928, 2015.
- [83] Y. Yang, W. Ching, and A. Misra. Higher-order continuum theory applied to fracture simulation of nanoscale intergranular glassy film. *Journal of Nanomechanics and Micromechanics*, 1(2):60–71, 2011.
- [84] F. dell’Isola, A. Della Corte, I. Giorgio, and D. Scerrato. Pantographic 2D sheets: discussion of some numerical investigations and potential applications. *International Journal of Non-Linear Mechanics*, pages 1–9, 2015. DOI:10.1016/j.ijnonlinmec.2015.10.010.
- [85] Y. Rahali, I. Giorgio, J. F. Ganghoffer, and F. dell’Isola. Homogenization à la Piola produces second gradient continuum models for linear pantographic lattices. *International Journal of Engineering Science*, 97:148–172, 2015.
- [86] Y. Rahali, I. Goda, and J.-F. Ganghoffer. Numerical identification of classical and nonclassical moduli of 3D woven textiles and analysis of scale effects. *Composite Structures*, 135:122–139, 2016.
- [87] A. Misra and P. Poursolhjouy. Granular micromechanics model for damage and plasticity of cementitious materials based upon thermomechanics. *Mathematics and Mechanics of Solids*, 2015. DOI:10.1177/1081286515576821.
- [88] A. Carcaterra, F. dell’Isola, R. Esposito, and M. Pulvirenti. Macroscopic description of microscopically strongly inhomogenous systems: A mathematical basis for the synthesis of higher gradients metamaterials. *Archive for Rational Mechanics and Analysis*, 218(3):1239–1262, 2015.
- [89] P. Neff, I.-D. Ghiba, A. Madeo, L. Placidi, and G. Rosi. A unifying perspective: the relaxed linear micromorphic continuum. *Continuum Mechanics and Thermodynamics*, 26(5):639–681, 2014.
- [90] V. A. Eremeyev and W. Pietraszkiewicz. Local symmetry group in the general theory of elastic shells. *Journal of Elasticity*, 85:125–152, 2006.
- [91] V. A. Eremeyev and W. Pietraszkiewicz. Material symmetry group of the non-linear polar-elastic continuum. *International Journal of Solids and Structures*, 49:1993–2005, 2012.
- [92] N. Challamel, A. Kocsis, and C.M. Wang. Discrete and non-local elastica. *International Journal of Non-Linear Mechanics*, 77:128–140, 2015.

- 790 [93] N. Roveri and A. Carcaterra. Damage detection in structures under travelling loads by the
791 Hilbert-Huang transform. *Mechanical System and Signal Processing*, 28:128–144, 2012.
- 792 [94] A. Bilotta and E. Turco. A numerical study on the solution of the Cauchy problem in elasticity.
793 *International Journal of Solids and Structures*, 46:4451–4477, 2009.
- 794 [95] A. Bilotta and E. Turco. Numerical sensitivity analysis of corrosion detection. *Mathematics and*
795 *Mechanics of Solids*, pages 1–17, 2014. DOI: 10.1177/1081286514560093.
- 796 [96] G. Alessandrini, A. Bilotta, A. Morassi, and E. Turco. Computing volume bounds of inclusions
797 by EIT measurements. *Journal of Scientific Computing*, 33(3):293–312, 2007.
- 798 [97] F. Buffa, A. Cazzani, A. Causin, S. Poppi, G.M. Sanna, M. Solci, F. Stochino, and E. Turco. The
799 Sardinia Radio Telescope: a comparison between close range photogrammetry and FE models.
800 *Mathematics and Mechanics of Solids*, in press:1–21, 2015. DOI: 10.1177/1081286515616227.
- 801 [98] F. Stochino, A. Cazzani, S. Poppi, and E. Turco. Sardinia Radio Telescope finite element model
802 updating by means of photogrammetric measurements. *Mathematics and Mechanics of Solids*, in
803 press:1–17, 2015. DOI: 10.1177/1081286515616046.

804 Antonio Cazzani
805 University of Cagliari
806 DICAAR — Dept. of Civil and Environmental Engineering and Architecture
807 2, via Marengo
808 I-09123 Cagliari
809 Italy Tel: +39-070-6755420; Fax: +39-070-6755418
810 e-mail, Corresponding author: antonio.cazzani@unica.it

811 Flavio Stochino
812 University of Sassari
813 DADU — Dept. of Architecture, Design and Urban Planning
814 Asilo Sella, 35, via Garibaldi
815 I-07041 Alghero (SS)
816 Italy
817 e-mail: fstochino@uniss.it

818 Emilio Turco
819 University of Sassari
820 DADU — Dept. of Architecture, Design and Urban Planning
821 Asilo Sella, 35, via Garibaldi
822 I-07041 Alghero (SS)
823 Italy
824 e-mail: emilio.turco@uniss.it